



OPEN ACCESS

EDITED BY

Haibo Wang,
Anhui Science and Technology
University, China

REVIEWED BY

Jianli Jimmy Zhao,
University of Alabama at Birmingham,
United States
Ahsan Riaz Khan,
Tongji University, China
Iqbal Ali Shah,
China Medical University, Taiwan

*CORRESPONDENCE

Lei Wang,
✉ wanglei@njucm.edu.cn
Yang Zhang,
✉ yangzhang@njucm.edu.cn

[†]These authors have contributed equally
to this work

RECEIVED 17 October 2025

REVISED 29 December 2025

ACCEPTED 12 January 2026

PUBLISHED 29 January 2026

CITATION

Xie S, Chang C, Tran TM, Zhou Z, Yu C,
Chen Y, Lin J, Xu J, Wang L and Zhang Y
(2026) Aerobic exercise inhibits oxidative
stress and improves diabetic cardiomyopathy
in rats by activating the
PROC/PAR1/Nrf2/HO-1 signaling pathway.
Front. Physiol. 17:1727186.
doi: 10.3389/fphys.2026.1727186

COPYRIGHT

© 2026 Xie, Chang, Tran, Zhou, Yu, Chen, Lin,
Xu, Wang and Zhang. This is an open-access
article distributed under the terms of the
[Creative Commons Attribution License \(CC
BY\)](https://creativecommons.org/licenses/by/4.0/). The use, distribution or reproduction in
other forums is permitted, provided the
original author(s) and the copyright owner(s)
are credited and that the original publication
in this journal is cited, in accordance with
accepted academic practice. No use,
distribution or reproduction is permitted
which does not comply with these terms.

Aerobic exercise inhibits oxidative stress and improves diabetic cardiomyopathy in rats by activating the PROC/PAR1/Nrf2/HO-1 signaling pathway

Sicong Xie^{1†}, Cheng Chang^{2†}, Thi Mai Tran¹, Zhiyi Zhou¹,
Chenshuo Yu¹, Yucheng Chen¹, Jiayin Lin¹, Jiaxuan Xu¹,
Lei Wang^{1*} and Yang Zhang^{1*}

¹Department of Rehabilitation Medicine, School of Acupuncture-Moxibustion and Tuina and School of Health Preservation and Rehabilitation, Nanjing University of Chinese Medicine, Nanjing, Jiangsu, China, ²Department of Cardiology, Kunshan Hospital of Traditional Chinese Medicine, Kunshan, Jiangsu, China

Diabetic cardiomyopathy (DCM) is a serious complication of end-stage diabetes that manifests as cardiac hypertrophy and heart failure. The present study performed a bioinformatics analysis to predict possible targets for aerobic exercise to improve DCM, and animal experiments were conducted to detect the relevant mechanisms. Oxidative stress (OS)-DCM-trained differentially expressed genes (DEGs) were retrieved from the GeneCards database and a Gene Expression Omnibus microarray dataset. Subsequently, a protein-protein interaction network was constructed to screen the hub genes of the OS-DCM-trained DEGs. In addition, a model of type 2 diabetes was established using streptozotocin and a high-fat diet. Rats were divided into the control, DCM and DCM plus exercise (DCME) groups. The DCME group underwent 8 weeks of moderate-intensity treadmill training. Assessment of cardiac function, myocardial enzymes and OS-related indicators in each group. Compared with the control group, the levels of BNP, CK-MB, c-TnT, LDH, MDA, LVEF, LVIDd, and LVIDs in the DCM group were significantly increased ($P < 0.05$), while SOD, GSH, and LVFS were significantly decreased ($P < 0.05$); The above indicators were significantly improved in DCME group rats ($P < 0.05$). In addition, the expression levels of target genes predicted to be associated with the aerobic exercise-induced improvement of DCM were detected and western blotting was used to determine the relevant signaling pathways. Bioinformatics analysis identified nine hub genes, which, according to Kyoto Encyclopedia of Genes and Genomes enrichment analysis, were mainly involved in "IL-17 signaling pathway," "TNF signaling pathway," "apoptosis" and "necroptosis." Aerobic exercise improved the heart function and myocardial enzymes of the rats in the DCM group, reduced myocardial damage, and inhibited fibrosis and OS. Detection of the nine core genes revealed that only protein C (PROC) met the predicted trend; PROC expression was lower in the DCM group than that in the control group and was higher in the DCME group than that in the DCM group ($P < 0.05$). Further confirmation using western

blotting suggested that aerobic exercise may improve DCM by activating the PROC/proteinase-activated receptor 1 (PAR1)/nuclear factor (erythroid-derived 2)-like 2 (Nrf2)/heme oxygenase-1 (HO-1) signaling pathway. In conclusion, aerobic exercise may mitigate DCM by activating the PROC/PAR1/Nrf2/HO-1 signaling pathway. These findings could pave the way for further investigations into how exercise might regulate OS and influences DCM progression, providing novel insights into its diagnosis and prognosis.

KEYWORDS

aerobic exercise, bioinformatics, diabetes cardiomyopathy, oxidative stress, PROC/PAR1/Nrf2/HO-1 signaling pathway

1 Introduction

Type 2 diabetes has become increasingly common worldwide (Hu et al., 2013) and cardiovascular issues are the predominant causes of death among individuals with diabetes. Diabetic cardiomyopathy (DCM), a cardiac condition associated with diabetes, occurs independent of coronary artery disease and hypertension (Chavali et al., 2013). DCM is characterized by structural and functional anomalies of the heart, including myocardial hypertrophy, interstitial fibrosis, cardiomyocyte apoptosis, and impairments in diastolic and systolic functions (Huynh et al., 2014). These hallmarks of DCM contribute to the onset of heart failure and an elevated risk of mortality among affected individuals (Tribouilloy et al., 2008). Clinical studies have shown that early identification and diagnosis and timely treatment are crucial for controlling the patient's condition (Chen et al., 2024).

DCM progression is also influenced by oxidative stress (OS) (Mohammed Yusof et al., 2018). Under physiological conditions, a number of cells continuously produce reactive oxygen species (ROS) such as superoxide radicals, hydroxyl radicals and hydrogen peroxide. ROS levels are regulated by several enzymes and physiological antioxidants including superoxide dismutase (SOD), glutathione (GSH) peroxidase, catalase and thioredoxin (Peng M. L. et al., 2022). However, excessive ROS production leads to OS, which negatively affects the functional integrity of biological tissues (Watanabe et al., 2010). Extensive experimental and clinical studies have shown that the production of ROS is increased in both types of diabetes, and that the onset of diabetes and its vascular complications, such as DCM, are associated with OS (Wu X. et al., 2022; Penckofer et al., 2002; Sano et al., 1998). Hyperglycemia, an important clinical manifestation of diabetes, is considered to produce ROS via the formation of advanced glycation end products (Mullarkey et al., 1990), altered polyol pathway activity (Williamson et al., 1993) and activation of NADPH oxidase via protein kinase C (Caturano et al., 2025).

Current studies on diabetic cardiomyopathy (DCM) have clearly established that oxidative stress is its core pathogenic mechanism: chronic hyperglycemia leads to excessive production of reactive oxygen species (ROS), which damages the myocardial antioxidant system and induces pathological abnormalities. Exercise can improve DCM by regulating oxidative stress through multiple pathways, such as reducing ROS production, upregulating the expression of superoxide dismutase (SOD), and activating the Keap1/Nrf2 pathway; among these, treadmill training not only enhances antioxidant capacity and reduces oxidative damage, but also alleviates DCM-related injury by

reversing hyperacetylation of mitochondrial enzymes via the FGF21-SIRT3 axis (Liu et al., 2021). In addition, treadmill training can improve left ventricular systolic function (Libonati et al., 1985), an effect associated with the regulation of oxidative stress (OS) and enhancement of myocardial energy metabolism; this is because aerobic exercise can promote mitochondrial biogenesis, optimize calcium handling in cardiomyocytes, and reduce myocardial fibrosis, thereby providing support for the maintenance or restoration of left ventricular systolic function (Li et al., 2025; Pei et al., 2024; Zhang et al., 2024). However, studies on the targets related to the free radical scavenging system in treadmill training-mediated cardiac function protection in DCM remain scarce.

Genomics, transcriptomics, proteomics and metabolomics have generated notable amounts of data that can be analyzed by combining bioinformatics and computer science, resulting in new methods for studying the molecular mechanisms of diseases (Guo et al., 2022). Due to the rapid advancement of gene chip technology, the identification of differentially expressed genes (DEGs) and the examination of their roles have emerged as novel approaches for investigating the molecular underpinnings of disease progression (Cui et al., 2024). Notably, exercise causes systemic changes across physiology and molecular pathways hard to assess via one factor, but bioinformatics-based high-throughput technologies can detect and integrate multi-dimensional exercise-induced changes (e.g., gene expression, protein abundance, metabolites) missed by traditional single-target research, aiding in filtering core factors and clarifying key molecular drivers of exercise's role in improving pathologies (Qi et al., 2024; Yan et al., 2017). The GSE129090 dataset was obtained in a study by Zhang et al. (2019a), which discovered that Bcl-2 was involved in the progression of cardiac hypertrophy. In addition, Grabowski et al. (2015) developed a rat model of left ventricular hypertrophy and investigated *Efcab6* as a potential candidate for left ventricular hypertrophy.

Regarding protein C (PROC), a potential effector, previous studies have shown that its activated form, activated protein C (APC), can induce the expression of protective genes in endothelial cells by activating the endothelial protein C receptor (O'Brien et al., 2006) or protease-activated receptor 1 (PAR1) in the receptor cascade (Esmon, 2006; Liu et al., 2012) further confirmed that PAR1 can activate the nuclear factor (erythroid-derived 2)-like 2 (Nrf2)/heme oxygenase-1 (HO-1) pathway, thereby exerting an anti-oxidative stress effect. These studies suggest that PROC and its related signaling pathways hold significant research value for alleviating oxidative stress in DCM.

Based on the hypothesis that "aerobic exercise improves diabetic cardiomyopathy (DCM) by regulating core genes, activating

signaling pathways and inhibiting oxidative stress (OS),” this study had two core objectives: first, to identify DCM-improving core genes related to aerobic exercise from multi-omics data via bioinformatics; second, to verify aerobic exercise’s therapeutic effect on DCM via animal experiments, detect the expression of selected core genes, explore underlying mechanisms, and provide potential molecular targets with hub genes as the key core for DCM intervention.

2 Materials and methods

2.1 Data source

GSE4616, GSE6880, GSE5606 and GSE4745 gene expression profiles were obtained from the Gene Expression Omnibus (GEO) database (<http://www.ncbi.nlm.nih.gov/geo>), a repository of high-throughput gene expression data, hybridization arrays, chips and microarrays (Lehti et al., 2007; Van Lunteren and Moyer, 2007; Glyn-Jones et al., 2007; Gerber et al., 2006). GSE4616 is a dataset based on the GPL81 platform (Affymetrix Murine Genome U74A Version 2 Array) and includes nine mouse myocardial samples, three control samples (males), three DCM samples (males) and three DCM-trained samples (males). The DCM-trained group underwent 1 h of treadmill training daily at a speed of 21 m/min and an incline of 2.5°. Following 1 day of acclimatization training on the rodent treadmill, the mice underwent the aforementioned training regimen 5 days/week. GSE6880 is a dataset based on the GPL341 platform (Affymetrix Rat Expression 230A Array) and includes six rat myocardial samples, three control samples (males) and three DCM samples (males). GSE5606 is a dataset based on the GPL1355 platform (Affymetrix Rat Genome 230 2.0 Array) and includes 14 rat myocardial samples, seven control samples (males) and seven DCM samples (males). GSE4745 is a dataset based on the GPL85 platform (Affymetrix Rat Genome U34 Array) and includes 24 rat myocardial samples, 12 control samples (males) and 12 DCM samples (males).

The BioBase package 2.68 (<https://bioconductor.org/packages/Biobase>) was used to normalize the data. According to the annotation information on the platform, the probes were labeled with gene symbols, multiple probes corresponding to the same gene were randomly selected to remove duplicates and a gene expression matrix was obtained.

2.2 OS-related gene datasets

The GeneCards database (<https://www.genecards.org/>) (Xu et al., 2023) was searched using the term ‘oxidative stress’ as a screening condition to collect genes related to OS.

2.3 Data preprocessing and integration

The standardized expression matrix from the microarray data was obtained from the GEO datasets and depicted through a box-line plot created using the ‘ggplot2’ package (<https://github.com/tidyverse/ggplot2>) in R 4.2.1 (<https://cran.r-project.org/>

bin/windows/base/old/4.2.1/). The probes were characterized using the annotation file of the dataset. Principal component analysis (PCA) was conducted to confirm the reproducibility and PCA visualizations were produced using the R package ‘ggplot2’.

The DEGs were screened using the ‘limma’ package in R (<https://bioinf.wehi.edu.au/limma/>). The cutoff criteria for statistical significance were an absolute \log_2 fold change (\log_2FC) > 1 and $P < 0.05$. A heat map and volcano plot of DEGs were constructed using the ‘ggplot’ package.

2.4 Screening of DEGs and OS-DEGs between DCM and control samples

The ‘limma’ package in R was used to screen for DEGs between DCM and control samples in the GSE4616, GSE6880, GSE5606 and GSE4745 datasets. $P < 0.05$ and $|\log_2FC| \geq 1$ were set as the threshold values for DEG identification. Subsequently, OS-related genes were retrieved from the GeneCards database. The OS-related gene list intersected with the previously identified DEGs. The results obtained by the two methods were combined to screen OS-DEGs and their differential expression was analyzed, identifying upregulated and downregulated OS-DEGs.

2.5 Protein-protein interaction (PPI) network analysis

A PPI network was established using the Search Tool for the Retrieval of Interacting Genes (STRING) database (<https://string-db.org>), which encompassed the majority of functional interactions among the proteins encoded for by OS-DEGs. Interactions that achieved a combined score of > 0.4 were considered statistically significant. The upregulated and downregulated OS-DEGs in the PPI network were examined using the STRING database.

2.6 Screening of DCM-trained DEGs and OS-DEGs

The ‘limma’ package in R was used to screen for DEGs between DCM and DCM-trained samples in the GSE4616 dataset. $P < 0.05$ and $|\log_2FC| \geq 1$ were set as the threshold values for DEG identification. Subsequently, lists of the aforementioned upregulated and downregulated OS-DEGs were generated, and these two lists were intersected with the DEGs between the DCM- and DCM-trained groups. The results obtained by the two methods were combined to screen OS-DCM-trained DEGs, and the differential expression of OS-DCM-trained DEGs was analyzed, identifying upregulated and downregulated OS-DCM-trained DEGs.

2.7 PPI network analysis of OS-DCM-trained DEGs

The PPI network was developed using the STRING database, which included nearly all functional interactions among proteins encoded by the OS-DCM-trained DEGs. Interactions with a

combined score of > 0.4 were regarded as statistically significant. Upregulated and downregulated OS-DCM-trained DEGs were examined using the STRING database.

2.8 Association analysis of OS-DCM-trained DEGs

The results of the OS-DCM-trained DEGs STRING analysis were visualized using Cytoscape (version 3.8.0) software (https://cytoscape.org/release_notes_3_8_0.html). The most closely connected modules from the PPI network (minimum required interaction score, 0.4) were selected for further analysis using the molecular complex detection plugin. The Cytoscape software plugin 'cytoHubba' (<https://apps.cytoscape.org/apps/cytohubba>) was used to filter hub genes from the entire PPI network, and to calculate the subgraph, information, local average connectivity, betweenness and closeness algorithms.

2.9 Gene ontology (GO) and kyoto encyclopedia of genes and genomes (KEGG) analyses

The Database for Annotation, Visualization, and Integrated Discovery (<https://davidbioinformatics.nih.gov>) (version 6.8) is a web-based analysis tool suite with an integrated discovery and annotation function that provides batch annotation and GO term enrichment analysis, in order to highlight the most relevant GO terms associated with related genes. The identified OS-DCM-trained DEGs were classified into three categories using GO analysis (ClusterProfiler package, <https://www.bioconductor.org/packages/release/bioc/html/clusterProfiler.html>): Molecular function (MF), biological process (BP) and cellular component (CC). Using Metascape (<http://metascape.org>), online KEGG enrichment analysis was also performed to predict the signaling pathways in which OS-DCM-trained DEGs may participate. Only terms with $P < 0.05$ were considered significant. The enriched pathways relevant to the current study are presented.

2.10 Experimental animals

Healthy 8-week-old male Sprague-Dawley rats ($n = 15$; weight, $\sim 200 \pm 20$ g; license SCXK 2019-0002; Hangzhou Medical College, Hangzhou, China) were housed at a constant temperature of $22^\circ\text{C} \pm 2^\circ\text{C}$ and 40%–50% humidity, under a 12-h light/dark cycle. Rats were fed standard rodent mash for 1 week and water *ad libitum*, and were then randomly separated into two groups: Control ($n = 5$) and type 2 diabetes mellitus (D2M; $n = 10$). The control group was fed a normal diet, whereas the DCM group was fed a high-fat diet (HFD) (cat. no. D12492; Research Diets, Inc.). All animal procedures were performed in accordance with the institutional guidelines and approved by the Institutional Animal Care and Use Committee and the Ethics Committee for Science Research of the Nanjing University of Chinese Medicine (Nanjing, China; approval no. 202401A029).

2.11 Experimental protocol

The methodology for inducing type 2 diabetes in rats has been described previously (Peng M. L. et al., 2022). Following a 4-week period of a consistent HFD, rats in the DCM group underwent a 12-h fast. Subsequently, a 2% solution of streptozotocin (STZ; Beijing Solarbio Science & Technology Co., Ltd.), prepared in 0.01 mM citric acid buffer at pH 4.1, was administered intraperitoneally at a dosage of 30 mg/kg body weight. The control group received a single intraperitoneal injection of the same volume of 0.01 mM citric acid buffer. After a 72-h interval, 200 μL blood samples were randomly drawn from the tail vein for analysis. If blood glucose levels reached > 11.1 mM, the DCM model was considered successfully established. A total of 10 rats were successfully modeled after 1 week of re-examination and removal of rats with substandard blood glucose. To measure blood glucose levels, ~ 200 μL blood was collected from the tail vein of rats weekly for a total of 2 weeks, and tested using a blood glucose meter (Roche Diagnostics). The amount of blood collected was less than the recommended maximum weekly blood collection amount, which is 7.5% of the circulating blood volume. Rats with successful modeling were randomly divided into the DCM ($n = 5$) and DCM plus exercise (DCME; $n = 5$) groups.

Ten successfully modeled rats were grouped using a completely randomized design: first, the rats were numbered consecutively from 1 to 10, then 10 non-repetitive random numbers (ranging from 1 to 10) were generated by computer. After sorting the random numbers, the rats corresponding to numbers 1–5 were assigned to the DCM group ($n = 5$), and those corresponding to numbers 6–10 were assigned to the DCME group ($n = 5$). The grouping was performed by independent personnel to avoid bias.

The rats assigned to the DCME group underwent an initial week of adaptive training, which consisted of running at a speed of 10 m/min for 15 min daily. This was followed by an 8-week regimen of moderate-intensity aerobic treadmill exercise as previously described (Yang et al., 2024). The exercise parameters included a speed of 15.2 m/min and a slope of 3, corresponding to an exercise intensity of $\sim 58.40 \pm 1.7\%$ of VO_2max . The sessions lasted 60 min per day and were conducted 5 days per week.

Studies have shown that 8 weeks of exercise training can achieve significant improvements in myocardial structure and function in diabetic cardiomyopathy (DCM) rats, providing sufficient time for the activation of relevant signaling pathways (Ma et al., 2025). Meanwhile, in rodent DCM models, moderate-intensity exercise has been widely confirmed to stably enhance myocardial antioxidant capacity (Wang and Feng, 2019). This intensity not only matches the clinically recommended exercise intensity for DCM patients but also avoids the risk of excessive cardiac load that may be induced by high-intensity exercise (Dias et al., 2018).

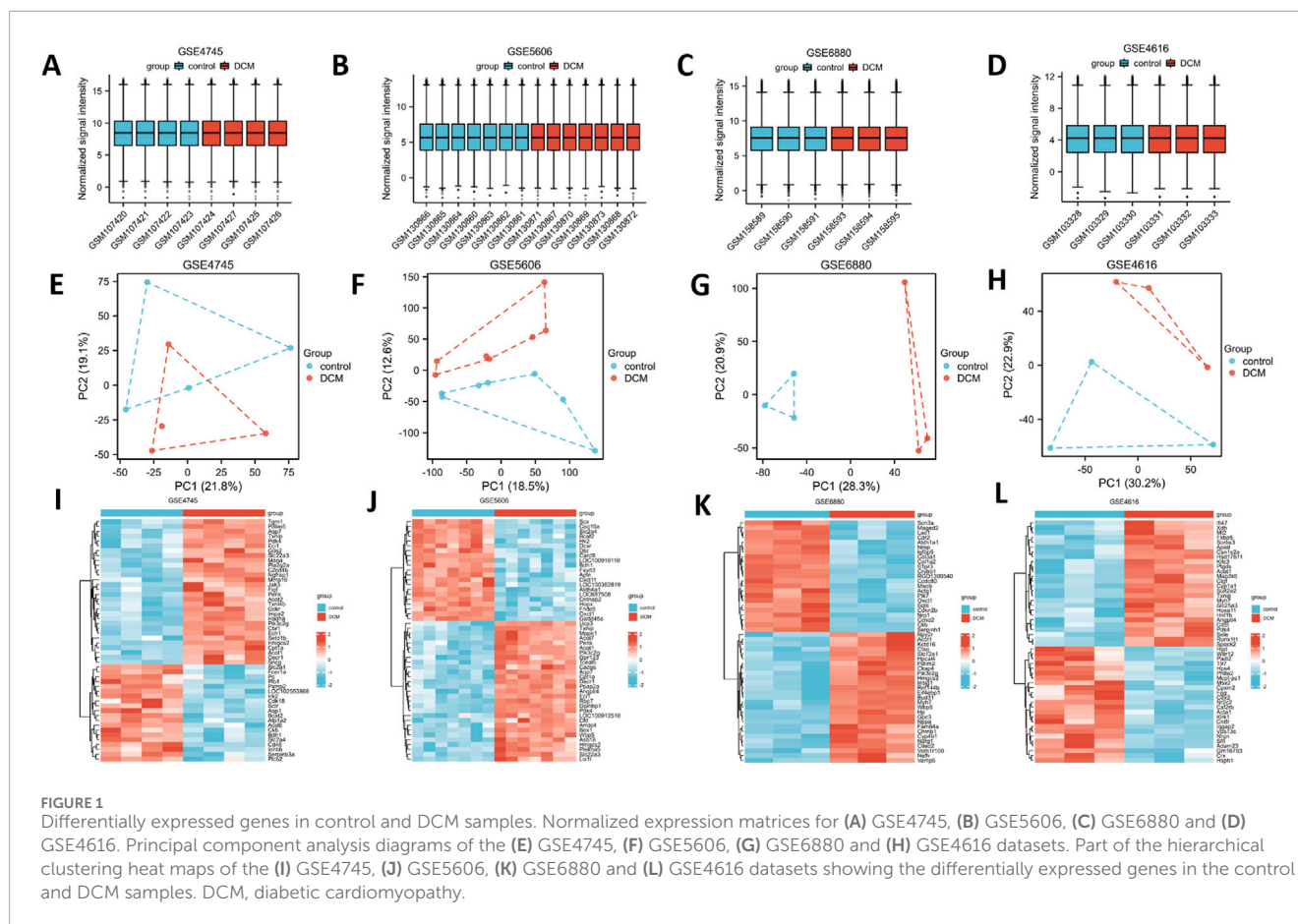
2.12 Insulin resistance test

Following a 12-h fasting period, serum samples were obtained from five rats each in the control group and the DCM group; briefly, 0.1 mL was collected from the tail vein of each rat, and centrifuged at $1,200 \times g$ for 10 min at 2°C – 8°C . The blood was allowed to clot for 30 min before serum collection. Fasting blood glucose (FBG) levels were measured using an automatic biochemical

TABLE 1 Primer sequences for reverse transcription-quantitative PCR.

Gene	Sequence, 5'-3'	References sequence
<i>Rattus FGG</i>		NM_012559.2
Forward	CCGCCTGACCTATGCCTACTTC	
Reverse	CATCCACCAGCCAGATCCATCC	
<i>Rattus HGD</i>		NM_001012145.1
Forward	CCATTGCTGACTTTGTGATCTTCCC	
Reverse	GAATCCACCTTGCTTTGCCTCATAG	
<i>Rattus PROC</i>		NM_012803.1
Forward	GAGCAACAGCGACAACGACATC	
Reverse	GTTCTTCTGCCATCCTTGACTTTG	
<i>Rattus TRADD</i>		NM_001100480.1
Forward	ACTGGAGTTGCGTGCTGGTG	
Reverse	GTCGGGCTTCTGGGCTAAGATG	
<i>Rattus GC</i>		NM_012564.3
Forward	TATGTGGAGCCGACGAATGATGAG	
Reverse	AAGTACAGCAGGAGCCAACCATAG	
<i>Rattus CCNA1</i>		NM_001011949.1
Forward	TGACCGTTCCAACCACCAACC	
Reverse	TGCTGCTACCAAGGAAGGAAGATAC	
<i>Rattus SPAG5</i>		NM_001044224.1
Forward	GGAAGTAGGCACCAAGGACAGTAC	
Reverse	GCAAGACAAGGGCGTTCAACAG	
<i>Rattus CASP8</i>		NM_022277.2
Forward	CGGTGCCTGTGCCTGATGAG	
Reverse	GCGTGGGATCTCGGTAGGAAAC	
<i>Rattus TOP2A</i>		NM_001393768.1
Forward	ACAGTCGCAAGAGGAAGCCATC	
Reverse	GAGGAGCCACAGTGTCATCTAAGTC	
<i>Rattus GAPDH</i>		NM_017008.4
Forward	AGTGCCAGCCTCGTCTCATA	
Reverse	ATCCGTTACACCGACCTTC	

FGG, fibrinogen γ chain; *HGD*, homogentisate 1,2-dioxygenase; *PROC*, protein C; *TRADD*, tumor necrosis factor receptor type 1-associated DEATH domain protein; *GC*, vitamin D-binding protein; *CCNA1*, cyclin A1; *SPAG5*, sperm-associated antigen 5; *CASP8*, caspase-8; *TOP2A*, DNA topoisomerase 2 α .



analyzer (Hitachi 7020; Hitachi, Ltd.) with a glucose oxidase kit (cat. no. ml059579; Shanghai Enzyme-linked Biotechnology Co., Ltd.). An enzyme-linked immunosorbent assay (ELISA) was used to measure fasting plasma insulin (FINS) (cat. no. HB549-Ra; Shanghai Hengyuan Biological Technology Co., Ltd.) using a microplate reader (WellScan MK3; LabSystems Diagnostics Oy). The insulin sensitivity index (ISI) and homeostatic model assessment of insulin resistance (HOMA-IR) were calculated using the following formulae: $ISI = -\log(FPG \times FINS)$; $HOMA-IR = (FPG \times FINS)/22.5$.

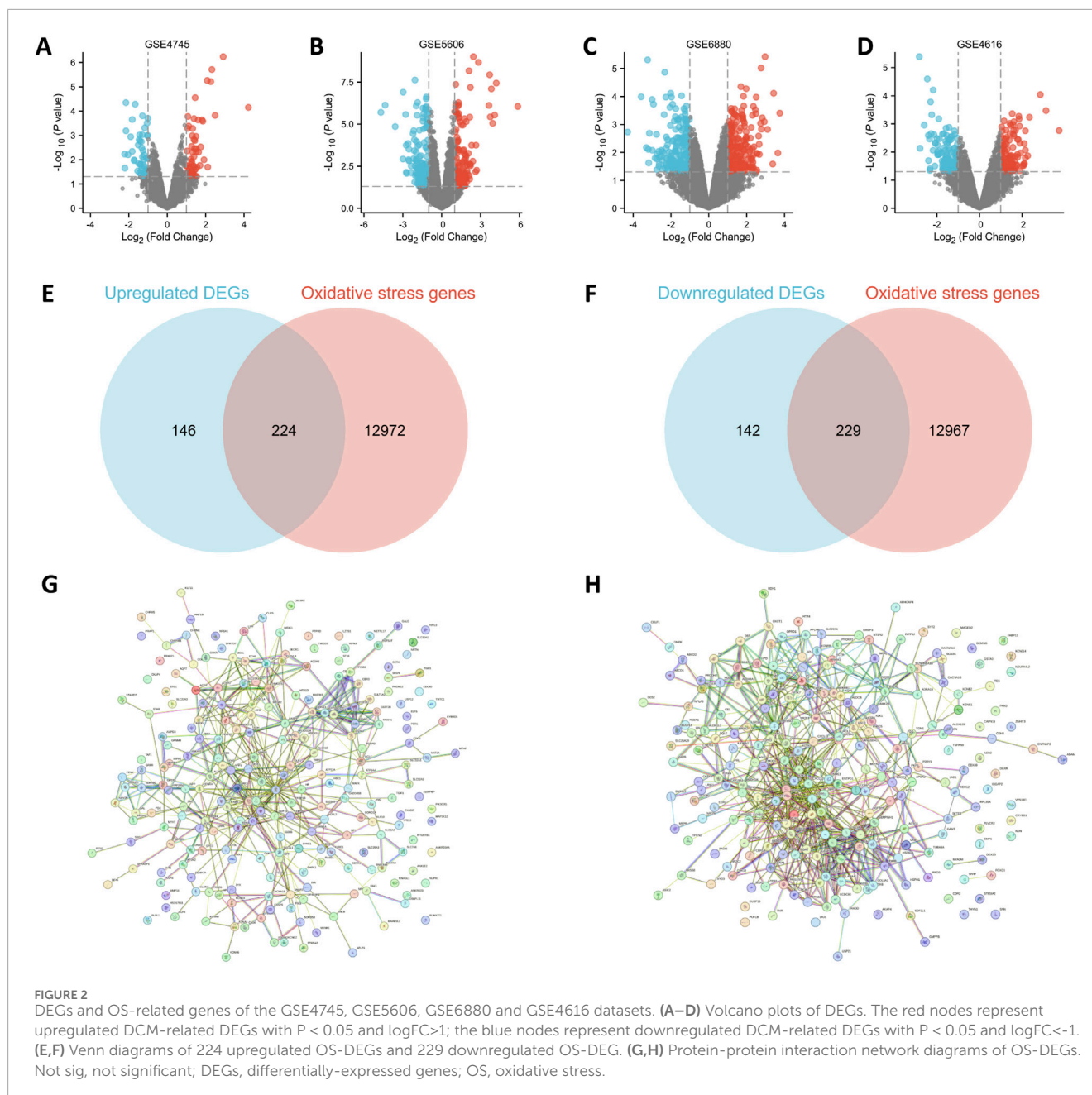
2.13 Echocardiogram

After 8 weeks of exercise, echocardiography was performed using a VINNO6 high-resolution imaging system [VINNO Technology (Suzhou) Co., Ltd.] following isoflurane anesthesia. The anesthesia protocol included induction with 4% isoflurane in 100% oxygen (1 L/min flow rate) using a precision evaporator and nasal cone, with anesthesia achieved within 2 min. Isoflurane concentration was maintained at 2% to ensure stable hemodynamics and to reduce cardiorespiratory depression. All procedures followed the institutional animal care guidelines and heating pads were used to maintain body temperature at 37 °C. Left ventricular ejection fraction (LVEF), left ventricular fractional shortening (LVFS), left ventricular internal diastolic dimension (LVIDd) and left ventricular internal dimension systole (LVIDs) were measured (Li et al., 2021).

2.14 Sample collection

After 8 weeks of exercise, all rats were euthanized. For euthanasia of Sprague-Dawley rats, sodium pentobarbital was administered intraperitoneally at a dose of 150 mg/kg. After sodium pentobarbital injection, death was confirmed by checking that rats were immobile, lacked a pain response when subjected to a toe pinch, were confirmed to lack a heartbeat and breathing, and exhibited dilated pupils. This protocol ensured rapid and humane euthanasia while complying with American Veterinary Medical Association guidelines (Gu et al., 2016).

In addition, for blood collection, pentobarbital sodium (50 mg/kg rat body weight; 1% solution concentration) was administered intraperitoneally to all rats in each group and the disappearance of corneal reflexes and stabilization of thoracic respiration were observed (Clifford et al., 2018). Subsequently, ~10 mL blood was obtained from the abdominal aorta from rats weighing 250 g, and the rats were immediately euthanized upon completion of this procedure, by sodium pentobarbital overdose. These blood samples were then centrifuged at $1,200 \times g$ for 15 min at 25 °C before the supernatant was collected. Upon collection of blood samples, the hearts of the rats were excised and rinsed with cold 0.9% saline. The surrounding vessels and connective tissues, along with the atrial and right ventricular tissues, were carefully removed. The procured cardiac tissue was then divided into two portions: Apical sections were swiftly frozen in liquid nitrogen (−196 °C).



for subsequent western blot analysis and the remaining tissue was preserved in 10% neutral-buffered formalin for fixation at room temperature for 4 h.

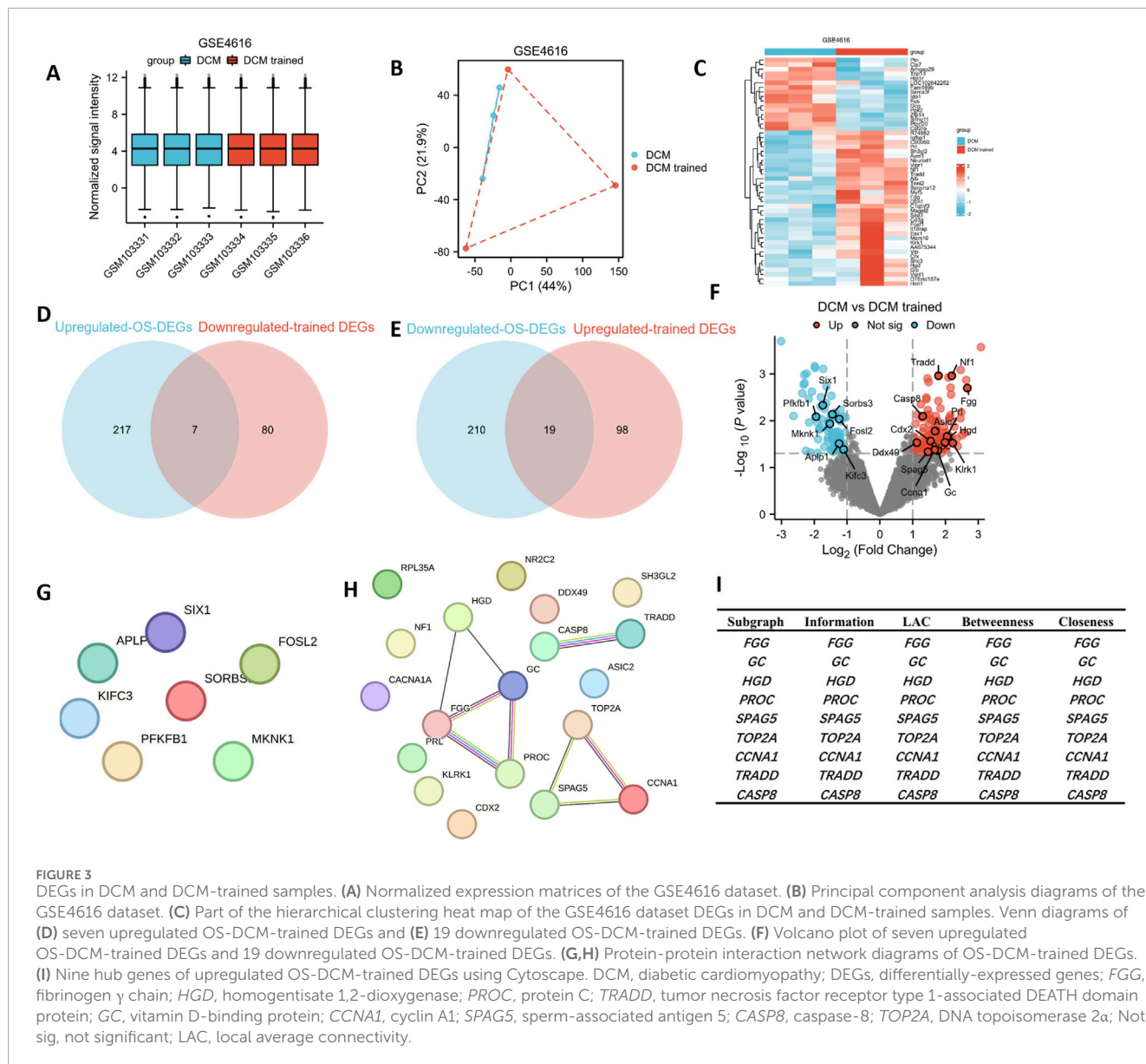
2.15 Histological evaluation

The excised heart tissues were embedded in paraffin and the tissue samples were sliced into 5- μ m sections for later staining with hematoxylin and eosin (H&E) at 90 °C for 30 min. Masson's trichrome staining was also performed on the 5- μ m sections to assess interstitial fibrosis (Zhang et al., 2019b). Images were obtained using a light microscope (BX51; Olympus Corporation) and a digital imaging system (DP71; Olympus Corporation). H&E- and

Masson's trichrome-stained tissue sections were examined at $\times 200$ magnification.

2.16 Assessment of biochemical parameters

Serum levels of brain natriuretic peptide (BNP; cat. no. SEKR-0058; Beijing Solarbio Science & Technology Co., Ltd.), creatine kinase MB (CK-MB; cat. no. SEKR-0059; Beijing Solarbio Science & Technology Co., Ltd.), cardiac troponin T (c-TnT; cat. no. SEKR-0047; Beijing Solarbio Science & Technology Co., Ltd.), malondialdehyde (MDA; cat. no. SP30131; Wuhan Saipai Biotechnology Co., Ltd.), lactate dehydrogenase (LDH; cat. no.



ml106660; Shanghai Enzyme-linked Biotechnology Co., Ltd.), GSH (cat. no. SP12673; Wuhan Saipei Biotechnology Co., Ltd.) and SOD (cat. no. SP12914; Wuhan Saipei Biotechnology Co., Ltd) were measured using ELISA kits, according to the manufacturer's instructions.

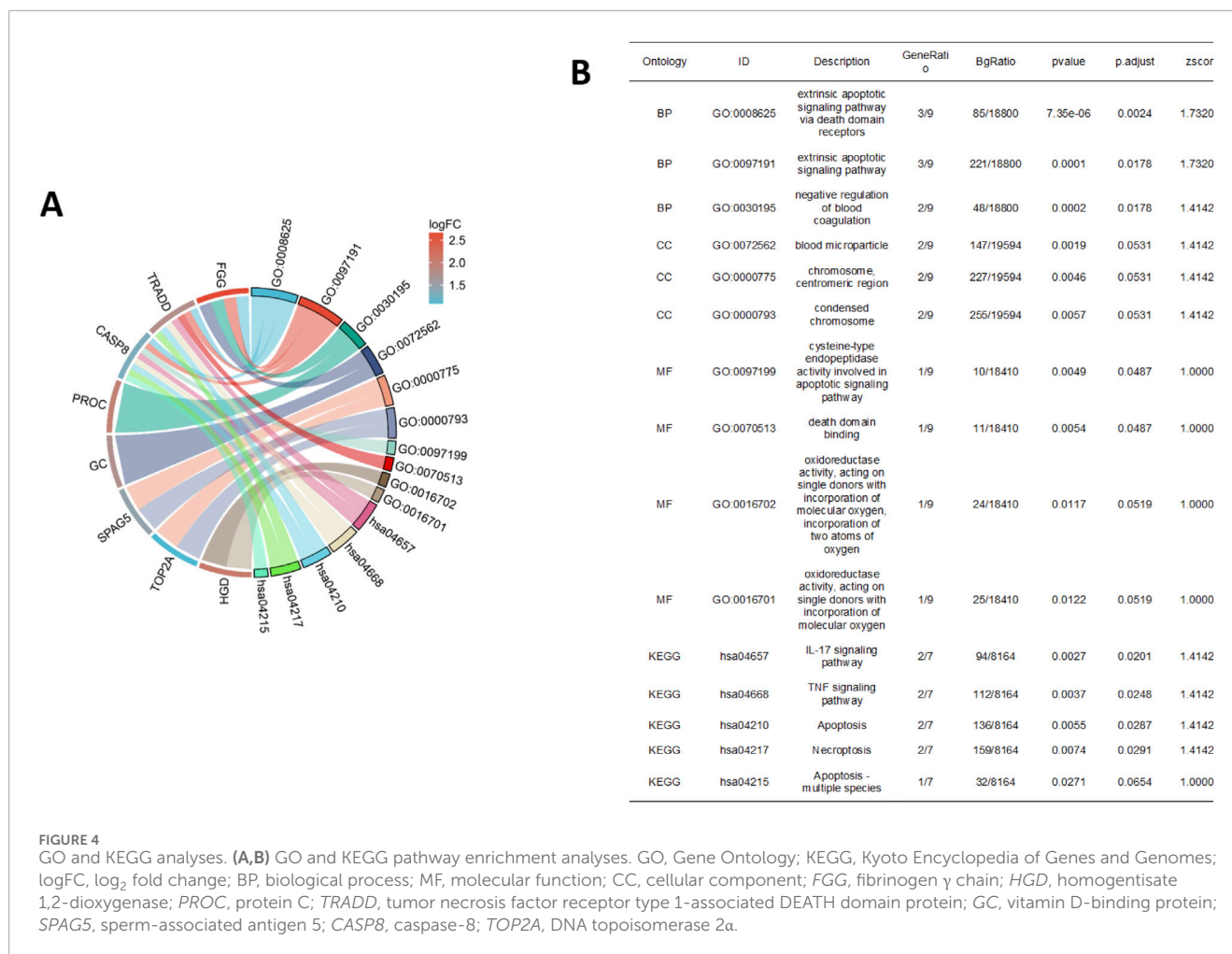
2.17 Reverse transcription-quantitative polymerase chain reaction (RT-qPCR)

Total RNA was extracted from the myocardium using an RNA extraction kit (cat. no. R1051; Guangzhou Dongsheng Biotech Co., Ltd.), and was used to synthesize cDNA using All-in-One first-strand cDNA Synthesis SuperMix for qPCR (TransGen Biotech Co. Ltd.) according to the manufacturer's protocol. A Tip Green qPCR SuperMix kit (TransGen Biotech Co., Ltd.) was used for qPCR according to the manufacturer's instructions, with GAPDH

used as the housekeeping gene. The thermocycling conditions were as follows: Pre-denaturation at 95 °C for 3 min, followed by 40 cycles of denaturation at 95 °C for 10 s followed by annealing/extension at 60 °C for 30 s. The mRNA expression levels of the target genes (Table 1) were calculated using the $2^{-\Delta\Delta Cq}$ method.

2.18 Concentrations of activated protein C (APC)

The concentration of APC in the tissue homogenate samples was determined using a commercially available Rat APC ELISA Kit (cat. no. XYR121; XYbio) according to the manufacturer's instructions. Before the test, the frozen serum samples were thawed and centrifuged again at 1,000 \times g for 15 min at 4 °C and all reagents in the ELISA kit were brought to room temperature. The serum supernatant was



added and the test performed according to the manufacturer's instructions.

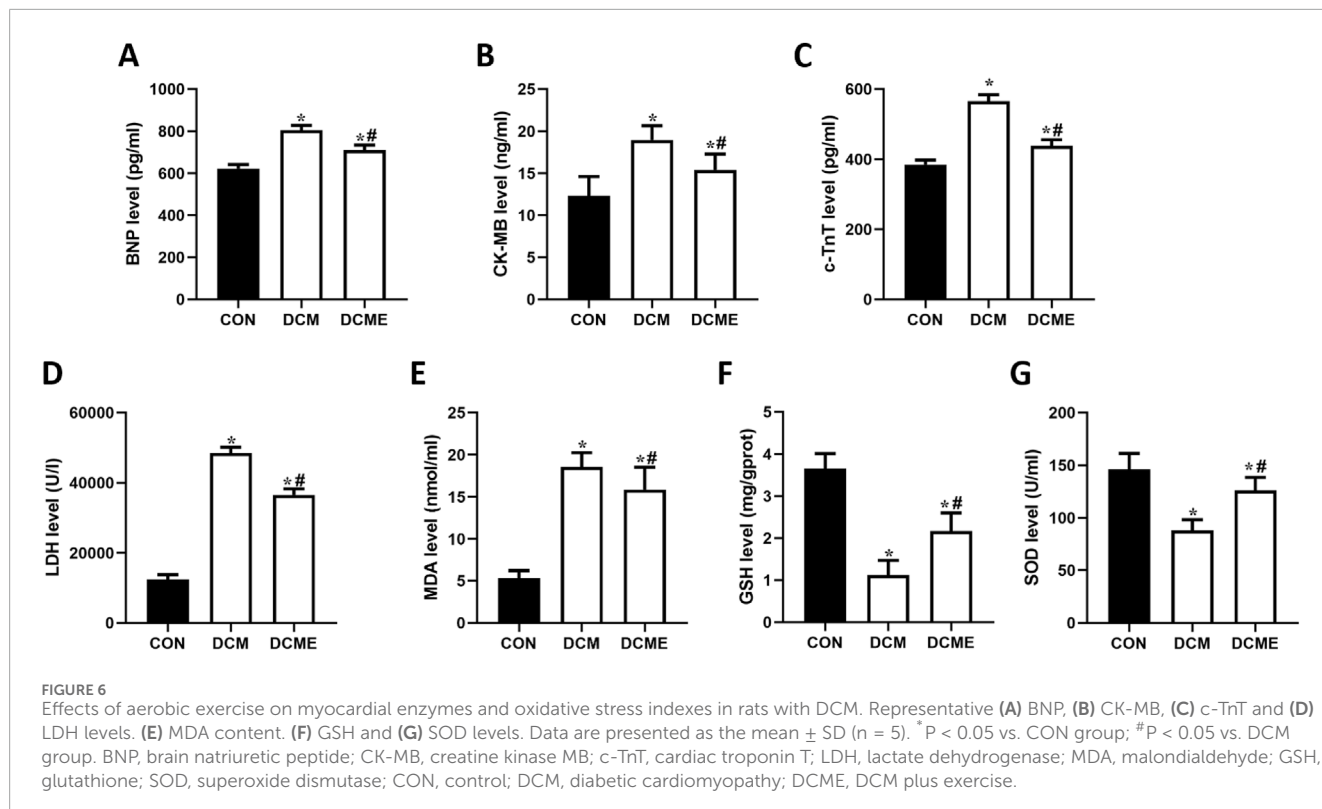
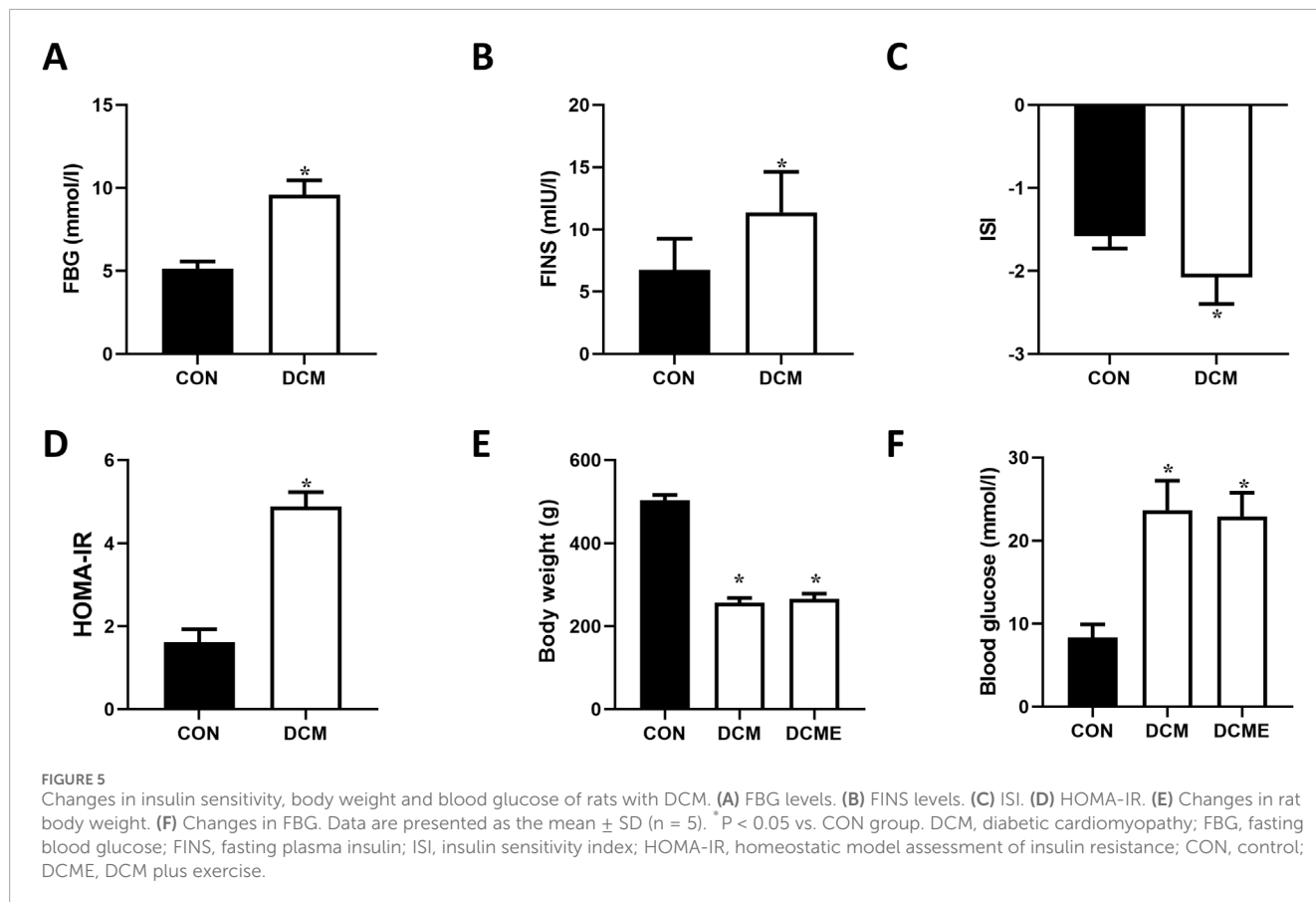
2.19 Western blot analysis

Western blot analysis was used to determine the protein levels in rat myocardial tissue samples. Briefly, mouse myocardial tissue samples were rapidly homogenized in 200 μ L RIPA lysis buffer (cat. no. P0013C; Beyotime Institute of Biotechnology) and protein levels were determined using the BCA method. Subsequently, 20 μ g protein/lane were separated by sodium dodecyl sulfate-polyacrylamide gel electrophoresis on a 10% gel, and the proteins were then transferred onto nitrocellulose membranes. The membranes were blocked with 5% non-fat dry milk in Tris-buffered saline for 60 min at room temperature and then incubated with anti-PROC (1:1,000; cat. no. MA5-35528; Thermo Fisher Scientific, Inc.), anti-tumor necrosis factor receptor type 1-associated DEATH domain protein (TRADD) (1:500) (cat. no. 703356; Thermo Fisher Scientific, Inc.), anti-caspase-8 (CASP8) (1:1,000; cat. no. MA1-41280; Thermo Fisher Scientific, Inc.), anti-cleaved CASP8 (1:1,000; cat. no. PA5-99435; Thermo Fisher Scientific, Inc.), anti-proteinase-activated receptor 1 (PAR1) (1:1,000; cat. no. PA5-116040; Thermo Fisher Scientific, Inc.), anti-nuclear factor (erythroid-derived 2)-like 2 (Nrf2; 1:1,000; cat. no.

PA5-27882; Thermo Fisher Scientific, Inc.), anti-heme oxygenase-1 (HO-1; 1:1,000; cat. no. PA5-77833; Thermo Fisher Scientific, Inc.) and anti-GAPDH (1:1,000; cat. no. MA5-35235; Thermo Fisher Scientific, Inc.) antibodies. The membranes were incubated overnight at 4 $^{\circ}$ C and washed three times before being incubated with the appropriate HRP-conjugated anti-rabbit (1:5,000; cat. no. 32460; Thermo Fisher Scientific, Inc.) or anti-mouse secondary antibodies (1:5,000; cat. no. 31431; Thermo Fisher Scientific, Inc.) for 60 min at room temperature. Enhanced chemiluminescent reagents (cat. no. 34098CN; Thermo Fisher Scientific, Inc.) were used to visualize protein bands. A digital gel imaging system was used to examine the protein expression levels (Alpha Imager2200 3.2; ProteinSimple).

2.20 Statistical analysis

All data are expressed as mean \pm SD and were analyzed using SPSS 21.0 (IBM, United States). Normality and homoscedasticity were assessed using the Shapiro-Wilk test and Levene's test, respectively. For data meeting the assumptions of normality and equal variance, an unpaired Student's t-test was employed for two-group comparisons, and one-way ANOVA followed by Tukey's post-hoc test was used for multiple group comparisons. A value of $P < 0.05$ was considered statistically significant.



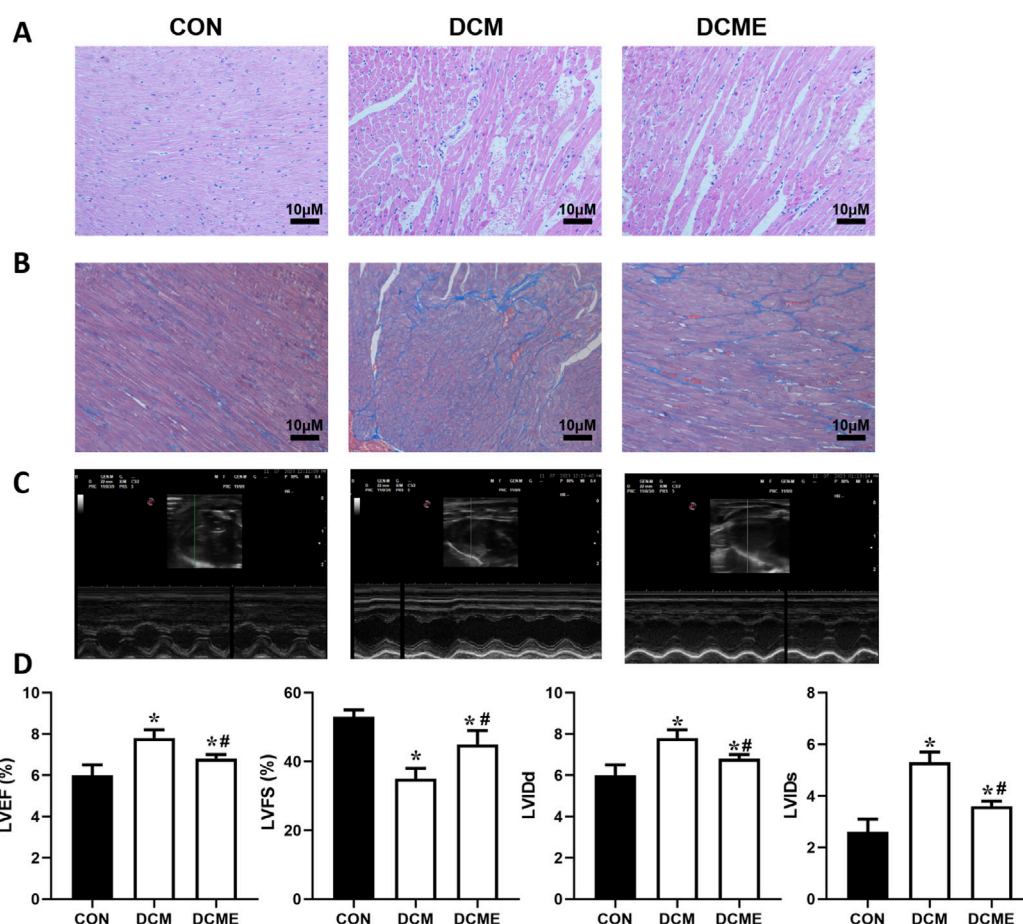


FIGURE 7

Effects of exercise training on histopathological and echocardiographic abnormalities in myocardial tissue. (A) H&E staining ($\times 200$ magnification) showed irregular arrangement of myocardial cells, uneven distribution of cytoplasm and ruptured myocardial fibers in the DCM group, whereas exercise training attenuated these histopathological changes. (B) Masson's trichrome staining ($\times 200$ magnification) showed irregular and noticeably increased interstitial collagen fibers (blue region) in the DCM group. (C) Echocardiography of rats in each group. (D) LVEF, LVFS, LVIDd and LVIDs in each group of rats. Data are presented as the mean \pm SD ($n = 3$). * $P < 0.05$ vs. CON group; # $P < 0.05$ vs. DCM group. H&E, hematoxylin and eosin; CON, control; DCM, diabetic cardiomyopathy; DCME, DCM plus exercise; LVEF, left ventricular ejection fraction; LVFS, left ventricular fractional shortening; LVIDd, left ventricular diastolic dimension; LVIDs, left ventricular systolic dimension.

3 Results

3.1 Screening of OS-DEGs between DCM and control groups

Four datasets were chosen to examine variations in gene expression between the DCM and control groups. The expression matrices for the GSE4616, GSE6880, GSE5606 and GSE4745 datasets were normalized, resulting in box plots that displayed the distribution trends as straight lines (Figures 1A–D). PCA was conducted on the four datasets to evaluate the consistency of the data within each group. The results indicated a high level of repeatability (Figures 1E–H). Figures 1I–L shows the partial gene heat maps of the four datasets.

After screening with the threshold of an adjusted $|\log FC| > 1$ and $P < 0.05$, 105 DEGs (58 upregulated and 47 downregulated in the DCM group) were identified in the GSE4745 dataset (Supplementary Table S1), 90 DEGs (45 upregulated and 45

downregulated in the DCM group) in the GSE5606 dataset (Supplementary Table S2), 382 DEGs (198 upregulated and 184 downregulated in the DCM group) in the GSE6880 dataset (Supplementary Table S3) and 238 DEGs (111 upregulated and 127 downregulated in the DCM group) in the GSE4616 dataset (Supplementary Table S4). Volcano plots of the DEGs in the four datasets are shown in Figures 2A–D. A total of 370 upregulated and 371 downregulated genes were identified by merging the upregulated and downregulated genes from the four datasets. The GeneCards database was used to cross-reference genes encoding OS proteins with the DEGs. A total of 13,196 related genes were identified in the GeneCards database (Supplementary Table S5), and 224 upregulated and 229 downregulated OS-DEGs were identified (Figures 2E,F). A PPI network was created by determining the interactions between upregulated and downregulated OS-DEGs. The PPI network showed that most OS-DEGs interacted with each other, and that the closer they were to the center of the network, the more genes they interacted with Figures 2G,H.

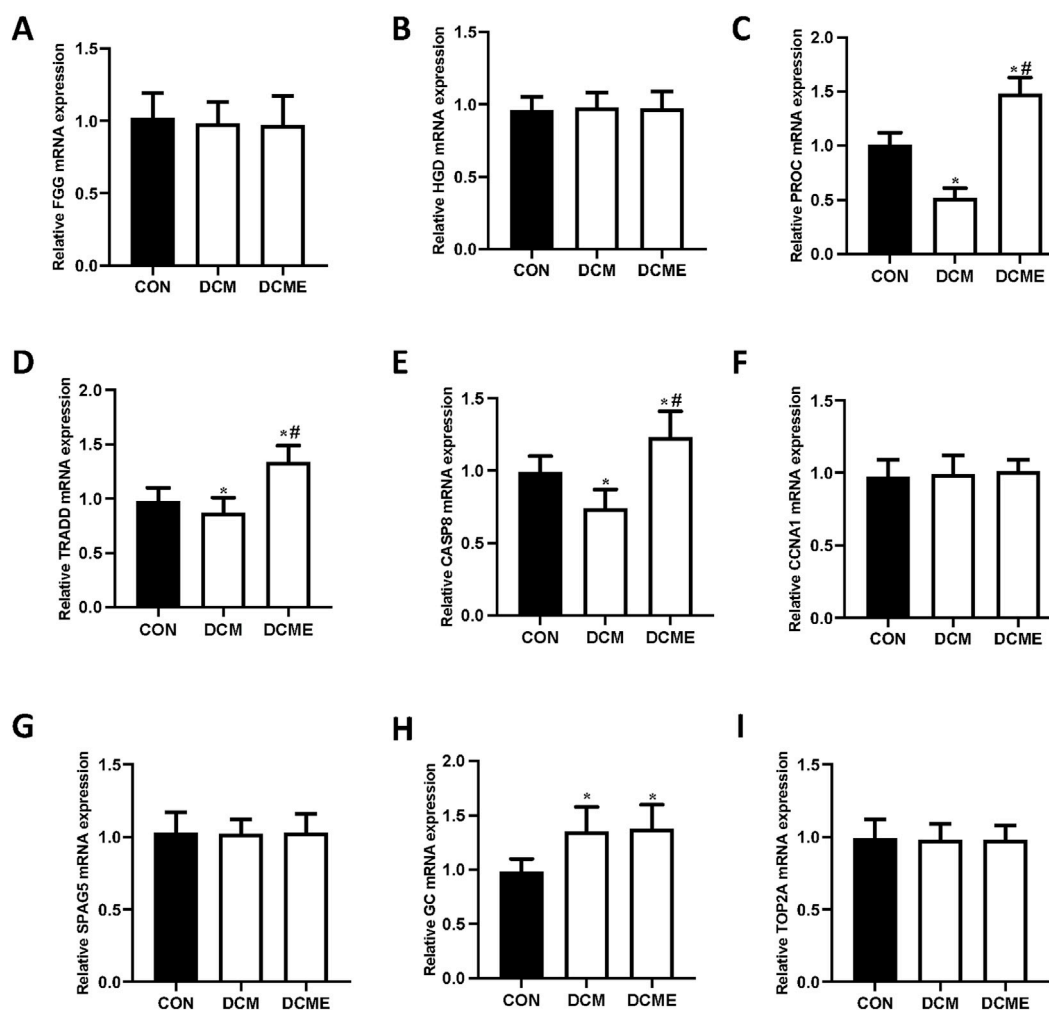


FIGURE 8

Effect of aerobic exercise on the expression levels of predicted genes in rats with DCM. Representative (A) *FGG*, (B) *HGD*, (C) *PROC*, (D) *TRADD*, (E) *CASP8*, (F) *CCNA1*, (G) *SPAG5*, (H) *GC* and (I) *TOP2A* mRNA expression levels. Data are presented as the mean \pm SD ($n = 3$). * $P < 0.05$ vs. CON group; # $P < 0.05$ vs. DCM group. CON, control; DCM, diabetic cardiomyopathy; DCME, DCM plus exercise; *FGG*, fibrinogen γ chain; *HGD*, homogentisate 1,2-dioxygenase; *PROC*, protein C; *TRADD*, tumor necrosis factor receptor type 1-associated DEATH domain protein; *GC*, vitamin D-binding protein; *CCNA1*, cyclin A1; *SPAG5*, sperm-associated antigen 5; *CASP8*, caspase-8; *TOP2A*, DNA topoisomerase 2 α .

3.2 Screening of OS-DCM-trained DEGs

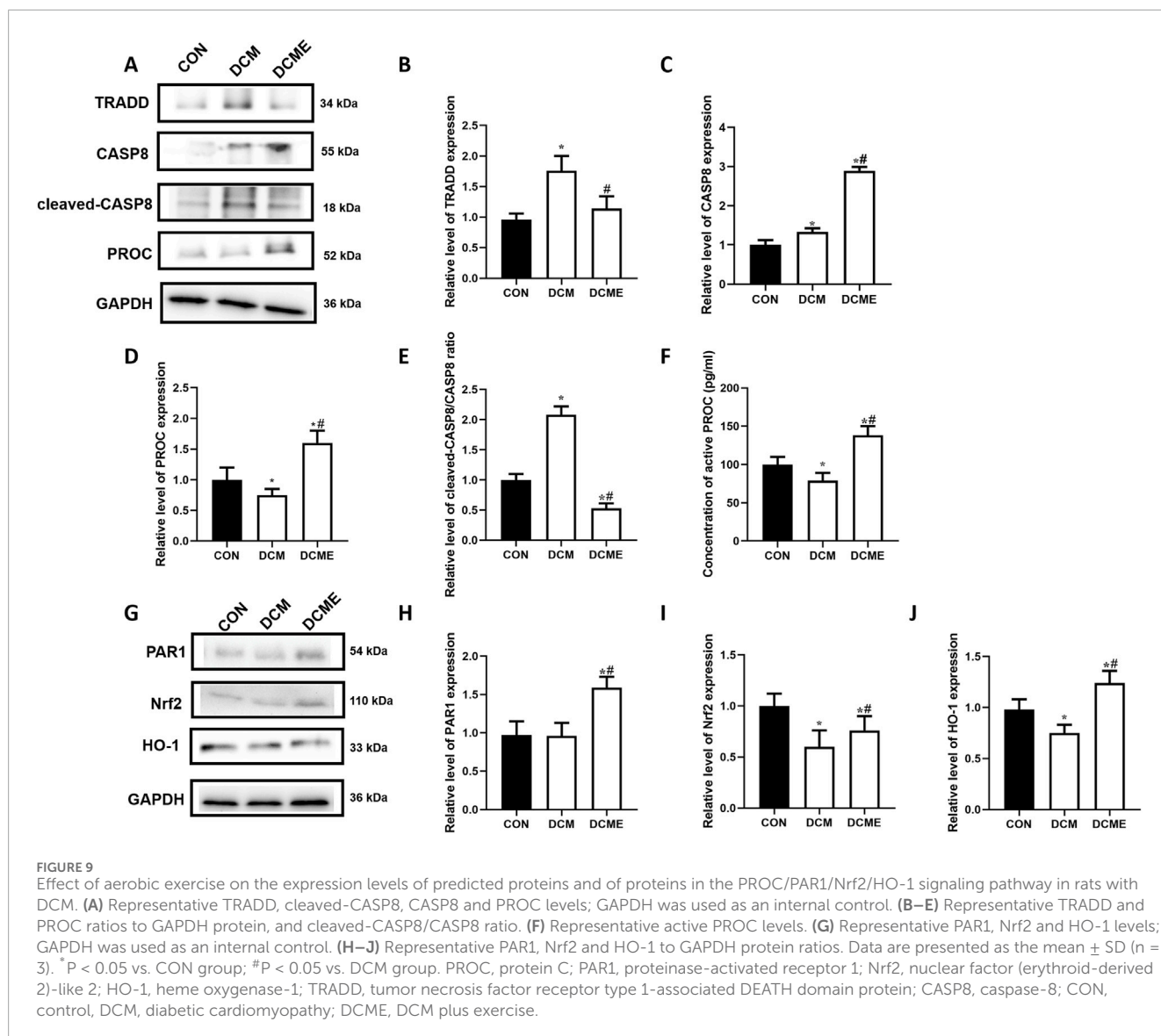
The GSE4616 dataset was the only one assessed in the present study that used aerobic exercise intervention on DCM. The expression matrices within the GSE4616 dataset were normalized, resulting in box plots that exhibited linear distribution trends (Figure 3A). To evaluate intragroup data reproducibility, PCA was conducted on the dataset, which revealed a high degree of repeatability (Figure 3B). Figure 3C shows a partial heat map of the dataset.

After screening using the thresholds of adjusted $|\log_{2}FC| > 1$ and $P < 0.05$, 204 DCM-trained DEGs (117 upregulated and 87 downregulated) were identified in the GSE4616 dataset (Supplementary Table S6). Subsequently, using a Venn diagram, the upregulated OS-DEGs were intersected with the downregulated DCM-trained DEGs, resulting in seven DEGs (Figure 3D). Simultaneously, 19 DEGs were identified by intersecting the

downregulated OS-DEGs with the upregulated DCM-trained DEGs (Figure 3E). A volcano plot illustrating the DEGs identified by OS-DCM training in the aforementioned datasets is shown in Figure 3F. The PPI network was created by determining the interactions between the downregulated (Figure 3G) and upregulated OS-DCM-trained DEGs (Figure 3H).

3.3 Identification of hub genes

The PPI results showed no association between the downregulated OS-DCM-trained DEGs (Figure 3G). Therefore, further research did not focus on these genes and instead investigated the upregulated OS-DCM-trained DEGs. The STRING analysis data were imported into Cytoscape and genes with scores were designated as hub genes. The top hub genes were identified using four different algorithms. An upshot diagram



of the results of these algorithms revealed nine common hub genes: Fibrinogen γ chain (*FGG*), homogentisate 1,2-dioxygenase (*HGD*), *PROC*, *TRADD*, vitamin D-binding protein (*GC*), cyclin A1 (*CCNA1*), sperm-associated antigen 5 (*SPAG5*), *CASP8* and DNA topoisomerase 2 α (*TOP2A*) (Figure 3I).

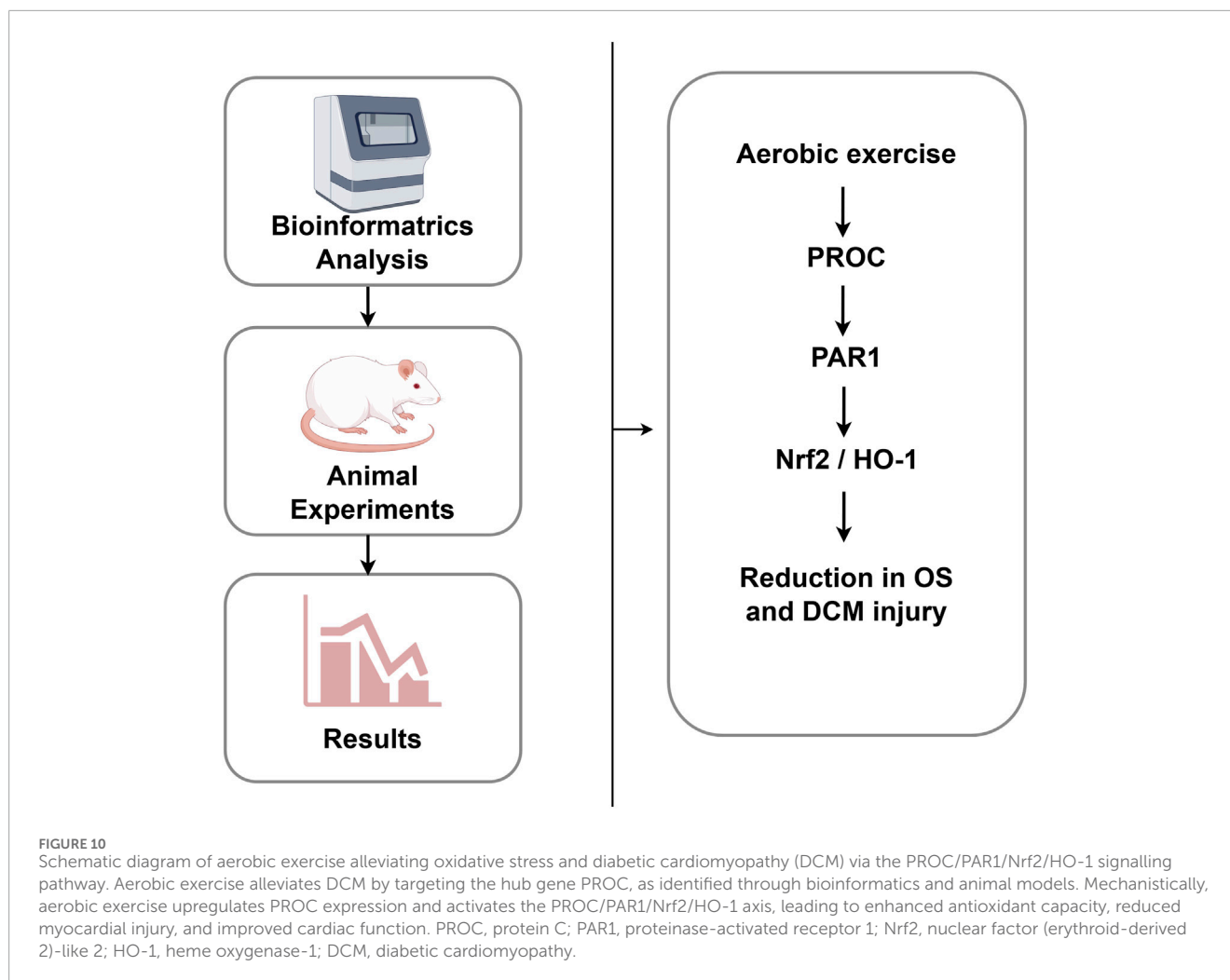
3.4 GO and KEGG analyses

GO and KEGG enrichment analyses of the upregulated OS-DCM-trained DEG hub genes were used to investigate their functions (Figures 4A,B). The ClusterProfiler package (<https://www.bioconductor.org/packages/release/bioc/html/clusterProfiler.html>) enriched GO function was used to determine the BP, CC and MF terms the hub genes were enriched in. The most enriched GO categories included “extrinsic apoptotic signaling pathway via death domain receptors,” “extrinsic apoptotic signaling pathway,” “cysteine-type endopeptidase activity involved

in apoptotic signaling pathway,” “oxidoreductase activity, acting on single donors with incorporation of molecular oxygen” and “oxidoreductase activity, acting on single donors with incorporation of molecular oxygen, incorporation of two atoms of oxygen.” Hub genes were mainly involved in apoptotic processes, such as “IL-17 signaling pathway,” “TNF signaling pathway,” “apoptosis” and “necroptosis” in the KEGG enrichment analysis.

3.5 Effects of aerobic exercise on body weight and blood glucose in diabetic rats

As shown in Figures 5A–D, rats in the DCM group exhibited significantly elevated FBG and FINS levels compared with those in the control group (both $P < 0.05$), along with significantly reduced ISI ($P < 0.05$) and increased HOMA-IR ($P < 0.05$). These findings suggested heightened insulin resistance in the DCM group,



demonstrating that the current animal model aligned with the characteristics of type 2 diabetes.

Changes in the body weight of the rats are shown in [Figure 5E](#). Compared with in the control group, the weights of rats in the DCM and DCME groups were significantly reduced ($P < 0.05$). Rats in the DCME group were heavier than those in the DCM group; however, the difference was not statistically significant. [Figure 5F](#) shows changes in blood glucose levels. Compared with those in the DCM group, blood glucose levels were not significantly different in the DCME group ($P > 0.05$).

3.6 Effects of aerobic exercise on serum myocardial enzymes levels

As shown in [Figures 6A–D](#), the serum levels of LDH, CK-MB, c-TnT and BNP were significantly elevated in the DCM group compared with those in the control group ($P < 0.05$). However, exercise training in the DCME group led to a significant reduction in LDH, CK-MB, c-TnT and BNP levels compared with those in the DCM group ($P < 0.05$).

3.7 Effects of aerobic exercise on myocardial OS in diabetic rats

Compared with that in the control group, the MDA content in the DCM group was significantly increased ($P < 0.05$), and the MDA content in the DCME group was significantly lower than that in the DCM group ($P < 0.05$), but was still significantly higher than that in the control group ($P < 0.05$) ([Figure 6E](#)). Furthermore, compared with those in the control group, the activities of SOD and GSH were significantly reduced in the DCM group ($P < 0.05$); however, compared with those in the DCM group, the SOD and GSH activities were significantly higher in the DCME group ($P < 0.05$) but remained significantly lower than those in the control group ($P < 0.05$) ([Figures 6F,G](#)).

3.8 Effects of aerobic exercise on myocardial pathological abnormalities

After H&E staining ([Figure 7A](#)), myocardial cells in the control group appeared to be compact and arranged in an orderly manner, with bright red cytoplasm and centrally located oval

nuclei. No dissolved muscle fibers, vacuolar degeneration or mononuclear cell infiltration were observed. However, in the DCM group, myocardial cells were disordered, and uneven cytoplasmic distribution, ruptured myocardial fibers and irregular nuclei were observed. The DCME group demonstrated reduced myocardial injury following moderate-intensity exercise training. Masson's trichrome staining (Figure 7B) revealed well-organized collagen fibers and no notable myocardial interstitial collagen deposition in the control group. By contrast, the DCM group displayed disorganized myocardial cells and a marked increase in interstitial collagen fibers within both intercellular and perivascular spaces. The DCME group showed reduced collagen fiber content compared with in the DCM group.

3.9 Effect of aerobic exercise on echocardiography

Compared with those in the control group, the LVEF and LVFS of the DCM group were significantly decreased, but the LVIDD and LVIDs were significantly increased, indicating impaired cardiac contractile function in the DCM group (Figures 7C,D). In addition, compared with those in the DCM group, the DCME group had significantly increased LVEF and LVFS, and decreased LVIDD and LVIDs, thus indicating improved cardiac contractile function (Cheng et al., 2022; Wu et al., 2024).

3.10 RT-qPCR detection of the expression of hub genes in heart tissues

RT-qPCR was used to examine the expression levels of *FGG*, *HGD*, *PROC*, *TRADD*, *GC*, *CCNA1*, *SPAG5*, *CASP8* and *TOP2A* in different samples (Figures 8A–I). According to bioinformatics predictions, compared with those in the control group, the target genes in the DCM group would be significantly reduced. By contrast, compared with in the DCM group, the target genes in the DCME group rats would be significantly elevated. Only *PROC*, *TRADD* and *CASP8* conformed to the predicted patterns.

3.11 Western blot detection of the expression of hub genes in heart tissues

Compared with that in the control group, the DCM group showed a significant decrease in *PROC* expression in cardiac tissues (Figures 9A,D). By contrast, compared with in the DCM group, the DCME group showed a significant increase in *PROC*. Compared with in the control group, *TRADD* expression was significantly elevated in cardiac tissue from the DCM group (Figures 9A,B). Conversely, *TRADD* expression was markedly reduced in the DCME group relative to the DCM group. Compared with in the control group, *CASP8* expression was significantly increased in cardiac tissue from the DCM group; *CASP8* expression was further increased in the DCME group relative to the DCM group (Figures 9A,C). Compared with in the control group, the cleaved-*CASP8*/*CASP8* ratio was significantly

increased in cardiac tissue from the DCM group, whereas it was decreased in the DCME group relative to the DCM group (Figures 9A,E).

3.12 Concentrations of serum APC

As shown in Figure 9F, compared with that in the control group, the APC content in the DCM group was significantly lower than that in the control group ($P < 0.05$), whereas the APC content in the DCME group was significantly higher than that in the DCM group ($P < 0.05$).

3.13 Western blot detection of the expression of PROC/PAR1/Nrf2/HO-1 signaling pathway proteins in heart tissues

As shown in Figures 9G–J, compared with those in the control group, the protein levels of Nrf2 and HO-1 were significantly reduced in the DCM group ($P < 0.05$), whereas the levels of PAR1, Nrf2 and HO-1 were significantly increased in the DCME group compared with those in the DCM group ($P < 0.05$).

4 Discussion

In this study, differentially expressed genes related to OS and DCM were screened from 4 GEO datasets. A PPI network was constructed, leading to the identification of 9 hub genes (e.g., *PROC*). Animal experiments confirmed that 8 weeks of aerobic exercise improved cardiac function, alleviated injury and OS in DCM rats, and only the expression of *PROC* was consistent with the prediction. Finally, it was verified that aerobic exercise exerts its effect by activating the *PROC*/*PAR1*/*Nrf2*/*HO-1* pathway. This study is the first to identify *PROC* as a key node in aerobic exercise-regulated DCM, filling the gap in genetic targets and providing a new direction for DCM intervention.

DCM is the leading cause of mortality in patients with diabetes, and no specific treatment is currently available in clinical practice (Livak and Schmittgen, 2001; Palomer et al., 2018). Regular exercise improves blood glucose control, lowers cardiovascular risk factors, aids in weight loss and improves overall wellbeing (Gilbert and Krum, 2015). The present study investigated the modulatory role and antioxidant potential of aerobic exercise in diabetes-induced myocardial injury.

Bioinformatics analysis was used to identify potential DEGs (She et al., 2025). The top hub genes were identified using four different algorithms. An upshot diagram of the results of these algorithms revealed nine common hub genes: *FGG*, *HGD*, *PROC*, *TRADD*, *GC*, *CCNA1*, *SPAG5*, *CASP8* and *TOP2A*. GO and KEGG enrichment analyses were used to investigate the functions of the upregulated OS-DCM-trained DEG hub genes. The most enriched GO categories included “extrinsic apoptotic signaling pathway via death domain receptors,” “extrinsic apoptotic signaling pathway” and “cysteine-type endopeptidase activity involved in apoptotic signaling pathway.” Hub genes were mainly involved in apoptotic processes, such as “IL-17 signaling pathway,” “TNF signaling

pathway,” “apoptosis” and “necroptosis” in the KEGG enrichment analysis. Some genes involved in DCM that are differentially expressed in response to OS have been studied previously. [American Diabetes Association \(2012\)](#) demonstrated that the activated nuclear catenin/c-Myc axis is responsible for oxidative cardiac impairment. In addition, [Liu et al. \(2017\)](#) discovered that excessive ROS production in DCM can activate the TLR-4/MyD-88/CASP8/CASP3 signaling pathway, leading to cardiomyocyte apoptosis. Subsequently, it was confirmed that aerobic exercise improved the expression of central DCM genes in rats.

In the present study, 8 weeks of treadmill exercise reduced blood glucose levels in diabetic rats; however, the improvement observed was not statistically significant compared with the DCM group. This suggested that 8 weeks of aerobic exercise can partially mitigate diabetes-induced hyperglycemia. In patients with type 2 diabetes, increased blood glucose is mainly associated with reduced sensitivity to insulin ([Liu et al., 2015](#); [Su et al., 2023](#)). In patients with diabetes, insufficient insulin sensitivity leads to persistently elevated blood glucose levels. Aerobic exercise enhances insulin sensitivity and facilitates the translocation of glucose transporter 4 to the cell membrane, promoting glucose uptake into cells, thereby lowering blood glucose levels ([Galicia-Garcia et al., 2020](#)). [Way et al. \(2016\)](#) also showed that the weight of diabetic rats in a D2M group was markedly decreased, along with a notable increase in FBG levels.

Cardiac function and myocardial enzyme levels were assessed in each group. Compared with those in the control group, the DCM group exhibited significantly elevated cardiac function and myocardial enzyme levels, indicating heart damage. These indicators significantly improved in the DCME group. Similarly, both H&E and Masson’s trichrome staining showed that aerobic exercise improved the myocardium of the DCM rats. [Wang et al. \(2019\)](#) used a HFD and STZ to induce DCM, and disrupted myocardial alignment and interstitial fibrosis were observed. In addition, [Wu S. et al. \(2022\)](#) demonstrated the presence of myocardial fibrosis in a rat model of DCM using Masson’s trichrome staining and Sirius red staining techniques. These previous findings indicated that STZ and HFD effectively replicate DCM in a rat model, and that aerobic exercise may improve cardiac function and enzyme levels in rats with DCM.

OS is associated with the occurrence and progression of pathological structural and functional changes in DCM ([Ren et al., 2020](#); [Faria and Persaud, 2017](#)). Under DCM conditions, antioxidant factors such as SOD and GSH are markedly reduced in the heart tissue, whereas reactive MDA generation, which is responsible for cellular OS, is notably increased ([Liao et al., 2017](#); [Wilson et al., 2018](#)). Thus, therapeutic molecules and methods that target intracellular OS represent potential DCM treatment strategies. The present study found that aerobic exercise reduced MDA levels in rat myocardial tissues, increased SOD and GSH levels, and thus conferred antioxidant stress resistance. [Kowluru and Mishra \(2015\)](#) reported that aerobic and resistance exercises may improve functional capacity and maximum load-carrying capacity, respectively. Furthermore, [Gomes et al. \(2020\)](#) reported that aerobic exercise can mitigate OS and cell death in mitochondria through the modulation of the Nrf2/glycogen synthase kinase 3 β signaling pathway, thus improving cognitive impairment observed in an aging model induced by D-galactose.

The predicted hub genes of the present study were tested and only the mRNA and protein expression levels of PROC were

revealed to match the trend predicted by bioinformatics analysis. Aerobic exercise may exert a cardioprotective effect by regulating PROC to improve DCM. APC, a serine protease belonging to the trypsin family, is produced during the initial phase of blood coagulation through limited proteolysis of PROC by thrombin, which binds to endothelial thrombomodulin ([Xie et al., 2024](#); [Esmon and Owen, 1984](#)). APC is a multifunctional enzyme that serves an important role in the regulation of blood coagulation, inflammation and apoptosis. It exhibits anti-inflammatory and cytoprotective properties that contribute to its diverse physiological effects ([Leon et al., 2022](#); [Biswas et al., 2024](#)). In the present study, compared with in the control group, the APC content in the DCM group was significantly decreased, whereas the APC content in the DCME group was significantly higher than that in the DCM group, indicating that aerobic exercise significantly increased the levels of APC, thus serving a role in alleviating DCM.

Previous studies have shown that APC induces the expression of protective genes in endothelial cells by activating endothelial protein C receptor ([O’Brien et al., 2006](#)) or the receptor cascade PAR1 ([Esmon, 2006](#)). Previous studies have shown that the PAR1 and PAR3 subtype receptors serve a role in neuroprotection, particularly in response to NMDA- and staurosporin-induced neuronal apoptosis ([Guo et al., 2004](#)). [Liu et al. \(2012\)](#) demonstrated that PAR1 can activate the Nrf2/HO-1 signaling pathway, thereby exerting antioxidant stress resistance. In addition, [Peng H. et al. \(2022\)](#) found that GF1 may reduce triptolide cytotoxicity in HL-7702 cells by activating the kelch-like ECH-associated protein 1 (Keap1)/Nrf2/antioxidant response element antioxidant pathway. In the present study, the results showed that compared with those in the control group, the protein levels of Nrf2 and HO-1 were significantly reduced in the DCM group, whereas PAR1 protein levels showed no significant alteration; by contrast, the protein levels of PAR1, Nrf2 and HO-1 were significantly increased in the DCME group compared with those in the DCM group.

According to this study, moderate-intensity aerobic exercise has clear guiding significance for the clinical exercise management of patients with DCM. It can inhibit OS by activating the PROC/PAR1/Nrf2/HO-1 pathway, thereby improving DCM. Clinically, the intensity parameters of this exercise are as follows: choose low-to-moderate impact exercises such as brisk walking and jogging, 3-5 times a week, 30-45 min each time, with heart rate maintained at 60%-70% of “220 minus age” ([Magutah et al., 2022](#)). This protocol is easy to implement, highly safe, and can help improve DCM. In conclusion, aerobic exercise may alleviate DCM through the aforementioned pathway; the study results lay a foundation for exploring how exercise regulates OS and affects DCM progression, and also provide new perspectives for disease diagnosis and prognosis.

However, the present study had certain limitations. Firstly, the GEO database was used to analyze the key genes involved in aerobic exercise-induced DCM improvement. Notably, the present study used a mixed dataset of rats (GSE4745, GSE6880, GSE5606) and mice (GSE4616) to analyze DEGs. Integrating data from these two species is an effective approach in bioinformatics and systems biology, especially when studying conserved biological mechanisms. This is because rats and mice have notable genetic and physiological similarities, which makes cross-species analysis valuable for improving the robustness and universality of research

results. When integrating rat and mouse diabetic cardiomyopathy (DCM) data, the core potential limitation of this study is that the inherent differences in DCM pathophysiological traits between the two species cannot be fully eliminated, which may compromise the accuracy of gene expression analysis. To address this, targeted strategies were adopted during data processing, including only genes significantly differentially expressed ($|\log_2FC| > 1$, $P < 0.05$) in both species to exclude interference from species-specific genes, prioritizing genes with consistent expression trends, and focusing on core, functionally conserved pathways (e.g., Nrf2/HO-1, PROC/PAR1 pathways) shared by the two species to improve conclusion reliability (Cheng et al., 2024; Sun et al., 2021). Future studies could further optimize the design by using a single species with an increased sample size or adopting advanced bioinformatics techniques to minimize inter-species differences and reduce potential biases (Li et al., 2024; Deng et al., 2024).

5 Conclusion

Diabetic cardiomyopathy (DCM) is closely linked to oxidative stress (OS). This study combined bioinformatics and animal experiments to confirm that 8 weeks of moderate-intensity aerobic exercise alleviates DCM in rats. Bioinformatics identified nine hub genes, with protein C (PROC) as the key target. Exercise upregulated PROC, activated the PROC/PAR1/Nrf2/HO-1 pathway, improved cardiac function, reduced myocardial injury markers and enhanced antioxidant capacity (Figure 10). Limitations include cross-species data integration. These findings highlight PROC as a novel target and aerobic exercise as a safe DCM intervention, providing insights for clinical management.

Data availability statement

The data generated in the present study may be requested from the corresponding authors.

Ethics statement

The animal study was approved by Institutional Animal Care and Use Committee of Nanjing University of Chinese Medicine. The study was conducted in accordance with the local legislation and institutional requirements.

Author contributions

SX: Conceptualization, Data curation, Formal Analysis, Investigation, Methodology, Project administration, Resources, Software, Supervision, Validation, Writing – original draft, Writing – review and editing. CC: Conceptualization, Data curation, Formal Analysis, Methodology, Project administration, Supervision, Validation, Writing – original draft. TT: Conceptualization, Data curation, Formal Analysis, Project administration, Validation, Writing – review and editing. ZZ: Conceptualization, Data curation, Investigation, Methodology, Software, Supervision, Writing –

original draft. CY: Conceptualization, Investigation, Software, Writing – original draft, Project administration, Resources, Visualization. YC: Conceptualization, Project administration, Writing – original draft, Formal Analysis, Methodology. JL: Conceptualization, Formal Analysis, Writing – original draft, Investigation, Software. JX: Conceptualization, Writing – original draft, Data curation, Methodology, Supervision. LW: Conceptualization, Data curation, Funding acquisition, Resources, Visualization, Writing – original draft, Writing – review and editing. YZ: Conceptualization, Data curation, Formal Analysis, Funding acquisition, Investigation, Methodology, Project administration, Resources, Software, Supervision, Validation, Visualization, Writing – original draft, Writing – review and editing.

Funding

The author(s) declared that financial support was received for this work and/or its publication. The present project was supported by the National Natural Science Foundation of China (grant no. 82302847) and the Jiangsu Province Basic Research Program (grant no. BK20241907).

Conflict of interest

The author(s) declared that this work was conducted in the absence of any commercial or financial relationships that could be construed as a potential conflict of interest.

Generative AI statement

The author(s) declared that generative AI was not used in the creation of this manuscript.

Any alternative text (alt text) provided alongside figures in this article has been generated by Frontiers with the support of artificial intelligence and reasonable efforts have been made to ensure accuracy, including review by the authors wherever possible. If you identify any issues, please contact us.

Publisher's note

All claims expressed in this article are solely those of the authors and do not necessarily represent those of their affiliated organizations, or those of the publisher, the editors and the reviewers. Any product that may be evaluated in this article, or claim that may be made by its manufacturer, is not guaranteed or endorsed by the publisher.

Supplementary material

The Supplementary Material for this article can be found online at: <https://www.frontiersin.org/articles/10.3389/fphys.2026.1727186/full#supplementary-material>

References

- American Diabetes Association (2012). Standards of medical care in diabetes–2012. *Diabetes Care* 1, S11–S63. doi:10.2337/dc12-s011
- Biswas, I., Giri, H., Panicker, S. R., and Rezaie, A. R. (2024). Thrombomodulin switches signaling and protease-activated receptor 1 cleavage specificity of thrombin. *Arterioscler. Thromb. Vasc. Biol.* 44, 603–616. doi:10.1161/ATVBAHA.123.320185
- Cheng, X., Tan, Y., Li, H., Huang, J., Zhao, D., Zhang, Z., et al. (2022). Fecal 16S rRNA sequencing and multi-compartment metabolomics revealed gut microbiota and metabolites interactions in APP/PS1 mice. *Comput. Biol. Med.* 151, 106312. doi:10.1016/j.compbiomed.2022.106312
- Caturano, A., Rocco, M., Tagliaferri, G., Piacevole, A., Nilo, D., Di Lorenzo, G., et al. (2025). Oxidative stress and cardiovascular complications in type 2 diabetes: from pathophysiology to lifestyle modifications. *Antioxidants (Basel)* 14, 72. doi:10.3390/antiox14010072
- Chavali, V., Tyagi, S. C., and Mishra, P. K. (2013). Predictors and prevention of diabetic cardiomyopathy. *Diabetes Metab. Syndr. Obes.* 6, 151–160. doi:10.2147/DMSO.S30968
- Chen, X., Chen, C., Tian, X., He, L., Zuo, E., Liu, P., et al. (2024). DBAN: an improved dual branch attention network combined with serum raman spectroscopy for diagnosis of diabetic kidney disease. *Talanta* 266, 125052. doi:10.1016/j.talanta.2023.125052
- Cheng, X., Huang, J., Li, H., Zhao, D., Liu, Z., Zhu, L., et al. (2024). Quercetin: a promising therapy for diabetic encephalopathy through inhibition of hippocampal ferroptosis. *Phytomedicine* 126, 154887. doi:10.1016/j.phymed.2023.154887
- Clifford, P. S., Ferguson, B. S., Jasperse, J. L., and Hill, M. A. (2018). Arteriolar vasodilation involves actin depolymerization. *Am. J. Physiol. Heart Circ. Physiol.* 315, H423–H428. doi:10.1152/ajpheart.00723.2017
- Cui, H., Hu, D., Xu, J., Zhao, S., Song, Y., Qin, G., et al. (2024). Identification of hub genes associated with diabetic cardiomyopathy using integrated bioinformatics analysis. *Sci. Reports* 14 (1), 15324. doi:10.1038/s41598-024-65773-z
- Deng, J., Liu, Q., Ye, L., Wang, S., Song, Z., Zhu, M., et al. (2024). The janus face of mitophagy in myocardial ischemia/reperfusion injury and recovery. *Biomed. Pharmacother.* 173, 116337. doi:10.1016/j.biopha.2024.116337
- Dias, K. A., Link, M. S., and Levine, B. D. (2018). Exercise training for patients with hypertrophic cardiomyopathy: JACC review topic of the week. *J. Am. Coll. Cardiol.* 72, 1157–1165. doi:10.1016/j.jacc.2018.06.054
- Esmon, C. T. (2006). Inflammation and the activated protein C anticoagulant pathway. *Semin. Thromb. Hemost.* 1, 49–60. doi:10.1055/s-2006-939554
- Esmon, C. T., and Owen, W. G. (1984). Identification of an endothelial cell cofactor for thrombin-catalyzed activation of protein C. *Proc. Natl. Acad. Sci.* 78, 2249–2252. doi:10.1073/pnas.78.4.2249
- Faria, A., and Persaud, S. J. (2017). Cardiac oxidative stress in diabetes: mechanisms and therapeutic potential. *Pharmacol. Ther.* 172, 50–62. doi:10.1016/j.pharmthera.2016.11.013
- Galicia-García, U., Benito-Vicente, A., Jebari, S., Larrea-Sebal, A., Siddiqi, H., Uribe, K. B., et al. (2020). Martin: pathophysiology of type 2 diabetes mellitus. *Int. J. Mol. Sci.* 21, 10.3390/ijms21176275
- Gerber, L. K., Aronow, B. J., and Matlib, M. A. (2006). Activation of a novel long-chain free fatty acid generation and export system in mitochondria of diabetic rat hearts. *Am. J. Physiol. Cell Physiol.* 291, C1198–C1207. doi:10.1152/ajpcell.00246.2006
- Gilbert, R. E., and Krum, H. (2015). Heart failure in diabetes: effects of anti-hyperglycaemic drug therapy. *Lancet* 385, 2107–2117. doi:10.1016/S0140-6736(14)61402-1
- Glyn-Jones, S., Song, S., Black, M. A., Phillips, A. R. J., Choong, S. Y., and Cooper, G. J. S. (2007). Transcriptomic analysis of the cardiac left ventricle in a rodent model of diabetic cardiomyopathy: molecular snapshot of a severe myocardial disease. *Physiol. Genomics* 28, 284–293. doi:10.1152/physiolgenomics.00204.2006
- Gomes, M. J., Pagan, L. U., Lima, A. R. R., Reyes, D. R. A., Martinez, P. F., Damatto, F. C., et al. (2020). Effects of aerobic and resistance exercise on cardiac remodelling and skeletal muscle oxidative stress of infarcted rats. *J. Cell Mol. Med.* 24, 5352–5362. doi:10.1111/jcmm.15191
- Grabowski, K., Riemenschneider, M., Schulte, L., Witten, A., Schulz, A., Stoll, M., et al. (2015). Fetal-adult cardiac transcriptome analysis in rats with contrasting left ventricular mass reveals new candidates for cardiac hypertrophy. *PLoS One* 10, e0116807. doi:10.1371/journal.pone.0116807
- Gu, Z., Eils, R., and Schlesner, M. (2016). Complex heatmaps reveal patterns and correlations in multidimensional genomic data. *Bioinformatics* 32, 2847–2849. doi:10.1093/bioinformatics/btw313
- Guo, H., Liu, D., Gelbard, H., Cheng, T., Insalaco, R., Fernández, J. A., et al. (2004). Activated protein C prevents neuronal apoptosis via protease activated receptors 1 and 3. *Neuron* 41, 563–572. doi:10.1016/j.neuron.2023.12.001
- Guo, Q., Zhu, Q., Zhang, T., Qu, Q., Cheang, I., Liao, S., et al. (2022). Integrated bioinformatic analysis reveals immune molecular markers and potential drugs for diabetic cardiomyopathy. *Front. Endocrinology* 13, 933635. doi:10.3389/fendo.2022.933635
- Hu, J., Pang, W., Chen, J., Bai, S., Zheng, Z., and Wu, X. (2013). Hypoglycemic effect of polysaccharides with different molecular weight of *Pseudostellaria heterophylla*. *BMC Complement. Altern. Med.* 13, 267. doi:10.1186/1472-6882-13-267
- Huynh, K., Bernardo, B. C., McMullen, J. R., and Ritchie, R. H. (2014). Diabetic cardiomyopathy: mechanisms and new treatment strategies targeting antioxidant signaling pathways. *Pharmacol. Ther.* 142, 375–415. doi:10.1016/j.pharmthera.2014.01.003
- Kowluru, R. A., and Mishra, M. (2015). Oxidative stress, mitochondrial damage and diabetic retinopathy. *Biochim. Biophys. Acta* 11, 2474–2483. doi:10.1016/j.bbdis.2015.08.001
- Lehti, T. M., Silvennoinen, M., Kivelä, R., Kainulainen, H., and Komulainen, J. (2007). Effects of streptozotocin-induced diabetes and physical training on gene expression of titin-based stretch-sensing complexes in mouse striated muscle. *Am. J. Physiol. Endocrinol. Metab.* 292, E533–E542. doi:10.1152/ajpendo.00229.2006
- Leon, G., Rehill, A. M., and Preston, R. J. S. (2022). The protein C pathways. *Curr. Opin. Hematol.* 29, 251–258. doi:10.1097/MOH.0000000000000726
- Li, X., Meng, C., Han, F., Yang, J., Wang, J., Zhu, Y., et al. (2021). Vildagliptin attenuates myocardial dysfunction and restores autophagy via miR-21/SPRY1/ERK in diabetic mice heart. *Front. Pharmacol.* 12, 634365. doi:10.3389/fphar.2021.634365
- Li, W., Liu, X., Liu, Z., Xing, Q., Liu, R., Wu, Q., et al. (2024). The signaling pathways of selected traditional Chinese medicine prescriptions and their metabolites in the treatment of diabetic cardiomyopathy: a review. *Front. Pharmacol.* 15, 1416403. doi:10.3389/fphar.2024.1416403
- Li, K., Li, S., Jia, H., Song, Y., Chen, Z., and Wang, Y. (2025). Aerobic exercise alleviates cardiac dysfunction correlated with lipidomics and mitochondrial quality control. *Antioxidants (Basel)* 14, 748. doi:10.3390/antiox14060748
- Liao, H., Zhu, J., Feng, H., Ni, J., Zhang, N., Chen, S., et al. (2017). Myricetin possesses potential protective effects on diabetic cardiomyopathy through inhibiting I κ B/NF κ B and enhancing Nrf2/HO-1. *Oxid. Med. Cell Longev.* 2017, 8370593. doi:10.1155/2017/8370593
- Libonati, J. R., Sabri, A., Xiao, C., Macdonnell, S. M., and Renna, B. F. (1985). Exercise training improves systolic function in hypertensive myocardium. *J. Appl. Physiol.* 111, 1637–1643. doi:10.1152/jappphysiol.00292.2011
- Liu, J., Hou, S., Tsai, C., Huang, C. Y., Yang, W. H., and Tang, C. H. (2012). Thrombin induces heme oxygenase-1 expression in human synovial fibroblasts through protease-activated receptor signaling pathways. *Arthritis Research and Therapy* 14, R91. doi:10.1186/ar3815
- Liu, Z., Wang, J., Qiu, C., Guan, G. c., Liu, X. h., Li, S. j., et al. (2015). Matrine pretreatment improves cardiac function in rats with diabetic cardiomyopathy via suppressing ROS/TLR-4 signaling pathway. *Acta Pharmacol. Sin.* 36, 323–333. doi:10.1038/aps.2014.127
- Liu, P., Su, J., Song, X., and Wang, S. (2017). Activation of nuclear β -catenin/c-Myc axis promotes oxidative stress injury in streptozotocin-induced diabetic cardiomyopathy. *Biochem. Biophys. Res. Commun.* 493, 1573–1580. doi:10.1016/j.bbrc.2017.10.027
- Liu, T., Li, X., Cui, Y., Meng, P., Zeng, G., Wang, Y., et al. (2021). Bioinformatics analysis identifies potential ferroptosis key genes in the pathogenesis of intracerebral hemorrhage. *Front. Neurosci.* 15, 661663. doi:10.3389/fnins.2021.661663
- Livak, K. J., and Schmittgen, T. D. (2001). Analysis of relative gene expression data using real-time quantitative PCR and the 2⁻(Delta Delta C(T)) method. *Methods (San Diego, Calif.)* 25, 402–408. doi:10.1006/meth.2001.1262
- Ma, X., Gao, H., Wang, Z., Zhu, D., Dai, W., Wu, M., et al. (2025). Beneficial effects of different types of exercise on diabetic cardiomyopathy. *Biomolecules* 15, 1223. doi:10.3390/biom15091223
- Magutha, K., Mbuthia, G., Akiruga, J. A., Haile, D., and Thairu, K. (2022). Effect of fixed 7.5 minutes' moderate intensity exercise bouts on body composition and blood pressure among sedentary adults with prehypertension in Western-Kenya. *PLOS Glob. Public Health* 2, e0000806. doi:10.1371/journal.pgph.0000806
- Mohammed Yusof, N. L., Zainalabidin, S., Mohd Fauzi, N., and Budin, S. B. (2018). Hibiscus sabdariffa (roselle) polyphenol-rich extract averts cardiac functional and structural abnormalities in type 1 diabetic rats. *Appl. Physiol. Nutr. Metab.* 43, 1224–1232. doi:10.1139/apnm-2018-0084
- Mullarkey, C. J., Edelstein, D., and Brownlee, M. (1990). Free radical generation by early glycation products: a mechanism for accelerated atherogenesis in diabetes. *Biochem. Biophys. Res. Commun.* 173, 932–939. doi:10.1016/s0006-291x(05)80875-7
- O'Brien, L. A., Gupta, A., and Grinnell, B. W. (2006). Activated protein C and sepsis. *Front. Biosci.* 11, 676–698. doi:10.2741/1827
- Palomer, X., Pizarro-Delgado, J., and Vázquez-Carrera, M. (2018). Emerging actors in diabetic cardiomyopathy: heartbreaker biomarkers or therapeutic targets? *Trends Pharmacol. Sci.* 39, 452–467. doi:10.1016/j.tips.2018.02.010

- Pei, W., Zhang, Y., Zhu, X., Zhao, C., Li, X., Lü, H., et al. (2024). Multitargeted immunomodulatory therapy for viral myocarditis by engineered extracellular vesicles. *ACS Nano* 18, 2782–2799. doi:10.1021/acsnano.3c05847
- Penckofer, S., Schwertz, D., and Florczak, K. (2002). Oxidative stress and cardiovascular disease in type 2 diabetes: the role of antioxidants and pro-oxidants. *J. Cardiovasc. Nurs.* 16, 68–85. doi:10.1097/00005082-200201000-00007
- Peng, M. L., Fu, Y., Wu, C. W., Zhang, Y., Ren, H., and Zhou, S. S. (2022a). Signaling pathways related to oxidative stress in diabetic cardiomyopathy. *Front. Endocrinology* 13, 907757. doi:10.3389/fendo.2022.907757
- Peng, H., You, L., Yang, C., Wang, K., Liu, M., Yin, D., et al. (2022b). Ginsenoside Rb1 attenuates triptolide-induced cytotoxicity in HL-7702 cells via the activation of Keap1/Nrf2/ARE pathway. *Front. Pharmacol.* 12, 723784. doi:10.3389/fphar.2021.723784
- Qi, S., Li, X., Yu, J., and Yin, L. (2024). Research advances in the application of metabolomics in exercise science. *Front. Physiol.* 14, 1332104. doi:10.3389/fphys.2023.1332104
- Ren, B., Zhang, Y., Liu, S., Cheng, X. J., Yang, X., Cui, X. G., et al. (2020). Curcumin alleviates oxidative stress and inhibits apoptosis in diabetic cardiomyopathy via Sirt1-Foxo1 and PI3K-Akt signalling pathways. *J. Cell. Mol. Med.* 24, 12355–12367. doi:10.1111/jcmm.15725
- Sano, T., Umeda, F., Hashimoto, T., Nawata, H., and Utsumi, H. (1998). Oxidative stress measurement by *in vivo* electron spin resonance spectroscopy in rats with streptozotocin-induced diabetes. *Diabetologia* 41, 1355–1360. doi:10.1007/s001250051076
- She, H., Zheng, J., Zhao, G., Du, Y., Tan, L., Chen, Z. S., et al. (2025). Arginase 1 drives mitochondrial cristae remodeling and PANoptosis in ischemia/hypoxia-induced vascular dysfunction. *Signal Transduct. Target Ther.* 10, 167. doi:10.1038/s41392-025-02255-2
- Su, M., Tang, T., Tang, W., Long, Y., Wang, L., and Liu, M. (2023). Astragalus improves intestinal barrier function and immunity by acting on intestinal microbiota to treat T2DM: a research review. *Front. Immunol.* 14, 1243834. doi:10.3389/fimmu.2023.1243834
- Sun, T. L., Li, W. Q., Tong, X. L., Liu, X. Y., and Zhou, W. H. (2021). Xanthohumol attenuates isoprenaline-induced cardiac hypertrophy and fibrosis through regulating PTEN/AKT/mTOR pathway. *Eur. J. Pharmacol.* 891, 173690. doi:10.1016/j.ejphar.2020.173690
- Tribouilloy, C., Rusinaru, D., Mahjoub, H., Tartière, J. M., Kesri-Tartière, L., Godard, S., et al. (2008). Prognostic impact of diabetes mellitus in patients with heart failure and preserved ejection fraction: a prospective five-year study. *Heart* 94, 1450–1455. doi:10.1136/hrt.2007.128769
- Van Lunteren, E., and Moyer, M. (2007). Oxidoreductase, morphogenesis, extracellular matrix, and calcium ion-binding gene expression in streptozotocin-induced diabetic rat heart. *Am. J. Physiol. Endocrinol. Metab.* 293, E759–E768. doi:10.1152/ajpendo.00191.2007
- Wang, C., and Feng, X. (2019). Exercise protects against diabetic cardiomyopathy by the inhibition of the endoplasmic reticulum stress pathway in rats. *J. Cell Physiol.* 234, 1682–1688. doi:10.1002/jcp.27038
- Wang, S. Q., Li, D., and Yuan, Y. (2019). Long-term moderate intensity exercise alleviates myocardial fibrosis in type 2 diabetic rats via inhibitions of oxidative stress and TGF- β 1/Smad pathway. *J. Physiol. Sci.* 69, 861–873. doi:10.1007/s12576-019-00696-3
- Watanabe, K., Thandavarayan, R. A., Harima, M., Sari, F. R., Gurusamy, N., Veeraveedu, P. T., et al. (2010). Role of differential signaling pathways and oxidative stress in diabetic cardiomyopathy. *Curr. Cardiol. Rev.* 6, 280–290. doi:10.2174/157340310793566145
- Way, K. L., Hackett, D. A., Baker, M. K., and Johnson, N. A. (2016). The effect of regular exercise on insulin sensitivity in type 2 diabetes. *Diabetes Metab. J.* 40, 253–271. doi:10.4093/dmj.2016.40.4.253
- Williamson, J. R., Chang, K., Frangos, M., Hasan, K. S., Ido, Y., Kawamura, T., et al. (1993). Hyperglycemic pseudohypoxia and diabetic complications. *Diabetes* 42, 801–813. doi:10.2337/diab.42.6.801
- Wilson, A. J., Gill, E. K., Abudalo, R. A., Edgar, K. S., Watson, C. J., and Grieve, D. J. (2018). Reactive oxygen species signalling in the diabetic heart: emerging prospect for therapeutic targeting. *Heart* 104, 293–299. doi:10.1136/heartjnl-2017-311448
- Wu, X., Zhou, X., Lai, S., Liu, J., and Qi, J. (2022a). Curcumin activates Nrf2/HO-1 signaling to relieve diabetic cardiomyopathy injury by reducing ROS *in vitro* and *in vivo*. *FASEB Journal Official Publication Fed. Am. Soc. Exp. Biol.* 36 (9), e22505. doi:10.1096/fj.202200543RRR
- Wu, S., Zhu, J., Wu, G., Ying, P., Bao, Z., Ding, Z., et al. (2022b). 6-Gingerol alleviates ferroptosis and inflammation of diabetic cardiomyopathy via the Nrf2/HO-1 pathway. *Oxid. Med. Cell. Longev.* 2022, 3027514. doi:10.1155/2022/3027514
- Wu, Q., Zhao, D., Leng, Y., Chen, C., Xiao, K., Wu, Z., et al. (2024). Identification of the hypoglycemic active components of *Lonicera japonica* thunb. and *Lonicera hypoglauca* Miq. by UPLC-Q-TOF-MS. *Molecules* 29, 4848. doi:10.3390/molecules29204848
- Xie, G., Xu, Z., Li, F., Kong, M., Wang, P., and Shao, Y. (2024). Aerobic exercise ameliorates cognitive disorder and declined oxidative stress via modulating the Nrf2 signaling pathway in D-galactose induced aging mouse model. *Neurochem. Res.* 49, 2408–2422. doi:10.1007/s11064-024-04164-2
- Xu, M., Zhou, H., Hu, P., Pan, Y., Wang, S., Liu, L., et al. (2023). Identification and validation of immune and oxidative stress-related diagnostic markers for diabetic nephropathy by WGCNA and machine learning. *Front. Immunol.* 14, 1084531. doi:10.3389/fimmu.2023.1084531
- Yan, X., Eynon, N., Papadimitriou, I. D., Kuang, J., Munson, F., Tirosh, O., et al. (2017). The gene SMART study: method, study design, and preliminary findings. *BMC Genomics* 18, 821. doi:10.1186/s12864-017-4186-4
- Yang, L., Lin, W., Yan, X., and Zhang, Z. (2024). Comparative effects of lifelong moderate-intensity continuous training and high-intensity interval training on blood lipid levels and mental well-being in naturally ageing mice. *Exp. Gerontol.* 194, 112519. doi:10.1016/j.exger.2024.112519
- Zhang, Y., Gago-Lopez, N., Li, N., Zhang, Z., Alver, N., Liu, Y., et al. (2019a). MacLellan: single-cell imaging and transcriptomic analyses of endogenous cardiomyocyte dedifferentiation and cycling. *Cell Discovery* 5, 30. doi:10.1038/s41421-019-0095-9
- Zhang, Y., Zhang, L., Fan, X., Yang, W., Yu, B., Kou, J., et al. (2019b). Captopril attenuates TAC-induced heart failure via inhibiting Wnt3a/ β -catenin and Jak2/Stat3 pathways. *Biomed. Pharmacother.* 113, 108780. doi:10.1016/j.biopha.2019.108780
- Zhang, Y., Zhu, L., Li, X., Ge, C., Pei, W., Zhang, M., et al. (2024). M2 macrophage exosome-derived lncRNA AK083884 protects mice from CVB3-induced viral myocarditis through regulating PKM2/HIF-1 α axis mediated metabolic reprogramming of macrophages. *Redox Biol.* 69, 103016. doi:10.1016/j.redox.2023.103016

Glossary

BNP	brain natriuretic peptide
BP	biological process
c-TnT	cardiac troponin T
CC	cellular component
CK-MB	creatinase kinase MB
DCM	diabetic cardiomyopathy
DCME	DCM plus exercise
DEGs	differentially expressed genes
ELISA	enzyme-linked immunosorbent assay
FBG	fasting blood glucose
FINS	fasting plasma insulin
GEO	Gene Expression Omnibus
GO	Gene Ontology
GSH	glutathione
HFD	high-fat diet
HO-1	heme oxygenase-1
HOMA-IR	homeostatic model assessment of insulin resistance
ISI	insulin sensitivity index
KEGG	Kyoto Encyclopedia of Genes and Genomes
LDH	lactate dehydrogenase
logFC	log ₂ fold change
LVEF	left ventricular ejection fraction
LVFS	left ventricular fractional shortening
LVIDd	left ventricular internal diastolic dimension
LVIDs	left ventricular internal dimension systole
MDA	malondialdehyde
MF	molecular function
Nrf2	nuclear factor (erythroid-derived 2)-like 2
OS	oxidative stress
PCA	principal component analysis
PPI	protein-protein interaction
PROC	protein C
ROS	reactive oxygen species
SOD	superoxide dismutase
STRING	Search Tool for the Retrieval of Interacting Genes
STZ	streptozotocin